ABSTRACT

BROWN, MICHELLE RENEE. Hybridized High Strength High Modulus Yarn Intercalated with Graphene Oxide Relationship at High Strain Rate. (Under the direction of Dr. Emiel DenHartog.)

Multiple studies have been performed to understand the relationship of fiber morphology, inter-fiber, intra-fiber friction and interfacial bonding to the properties of fibers and associated components in ballistic protective systems for personnel and equipment. Understanding these complex relationships and their roles in controlling or influencing final properties is critical to design and development efforts. This research focuses on testing high performance yarn with the introduction of graphene oxide (GO) and high strength high modulus PVA to improve impact performance.

Testing of protective systems for personnel and equipment is primarily performed in final products through several design iterations. Intermediate testing is not performed or accepted in the industry as standards do not exist for the methods and the influence of the intermediate form is not well characterized. In this research an effort was made to evaluate high strength fibers, yarns and fabrics with additional evaluation methods that may reduce the need for end item testing during development of new high performance materials and products.

Hybridization of two different high strength yarns, Kevlar KM2 Plus® and PVA was completed by commingling the different fibers or twisting them into one yarn, with further treatment of this yarn by graphene oxide. Testing was performed at low strain rate (tensile testing) and high strain rate (Split Hopkinson Pressure Bar (SHPB) or sonic modulus) to compare the change in modulus as a function of strain rate. Evaluation of the contribution of

graphene oxide was performed at the different strain rates but was also determined through coefficient of friction testing.

The results showed effects on toughness, tribology, strain rate behavior and failure modes with the introduction of PVA (either commingled or twisted) and GO. Twisting of the yarn consistently increased the performance of yarn compared to the commingled yarn. In fabric form the GO did show a greater contribution to improved strength. The different methodologies yielded differing values for the modulus with dynamic modulus more equal to initial tangent modulus and quasi-static modulus more related to a longer section of the stress strain curve.

The main conclusions from this research are commingling of two high strength high modulus yarns does not necessarily translate into improved tenacity, toughness or modulus. This was seen across each methodology. GO does not contribute in a tribological manner to increase energy absorption introduced on the yarn surface. High strain rate testing using different test methods does not always yield a correlation from one test to another. Use of high strain rate testing may require sample validation to compare one test method to another as sample geometry and configuration were shown to make a difference in test results.

Hybridized High Strength High Modulus Yarn Intercalated with Graphene Oxide Relationship at High Strain Rate

by

Michelle Brown

Dissertation submitted to the Graduate Faculty of
North Carolina State University
in partial fulfillment of the
requirements for the degree of
Doctor of Philosophy

Fiber and Polymer Science

Raleigh, North Carolina

2017

APPROVED BY

_____	_____
Dr. Emiel A. DenHartog Committee Chair	Dr. Stephen Michielsen
_____	_____
Dr. Wei Gao	Dr. Jagannadham Kasichainula

BIOGRAPHY

Michelle R. Brown was born in Greenville, S.C. in September 1957 and remained there graduating from Greenville Senior High School. In the fall of 1975 she began her college career at Charleston Southern University. In the spring of 1979 she received a Bachelor of Science degree in Chemistry from Charleston Southern University. Upon graduation, Michelle worked for Nutricia as Manager of the Chemistry Laboratory. She left Nutricia and worked for Digital Equipment Corporation as a Senior Research Scientist in the R&D facility. She moved to Greensboro N.C. in 1993 and worked for BGF Industries as Senior Technical Engineer. She continues to be employed at BGF Industries, Inc. In 2012 she received her Master of Science degree in Materials Science and Engineering from North Carolina State University. Continuing her education she pursued her Ph. D in Fiber and Polymer Science at North Carolina State University.

AKNOWLEGMENTS

I would like to thank my committee for your guidance, patience and support through my graduate studies. Dr. DenHartog as the chair for the committee I thank you for always encouraging me and offering support in all my testing. Dr. Michielsen: You have inspired me to question what is known about a problem because the solution will depend on what we know and what we can know. Dr. Kashichainula I specifically thank you for all your encouragement, understanding and willingness to answer any questions. Dr. Gao I thank you for your support in providing the graphene oxide, your kindness and willingness to be a part of my committee.

I wish to also thank Dr. Mark Pankow for guidance in using the Split Hopkinson Pressure bar and Shreyas Joglekar for his assistance in using the SHPB and patience in days of testing.

I also wish to thank Lawson Hemphill and Ms. Filiz Avsar for her invaluable assistance with their test equipment.

I owe special thanks to Jacen Busick of BGF as he was my proctor and equipment master throughout my graduate studies. Additionally I would like to thank my family for their support, patience and understanding in this process.

TABLE OF CONTENTS

LIST OF TABLES ..... **vi**

LIST OF FIGURES ..... **vii**

1 INTRODUCTION **1**
1.1 Purpose of Research *4*
1.2 Research Questions *4*

2 LITERATURE REVIEW **5**
2.1 Overview of Protective Systems and Current System configuration *5*
2.2 The Mechanism of Energy Absorption *7*
2.2.1 Fiber Surface Modification 7
2.2.2 Utilization of nanoparticles for nanoindentation and nanoscratch 13

3 BALLISTIC PROPERTY TEST METHODOLOGY **17**
3.1 High Strain Rate Testing with Split Hopkinson Pressure Bar *17*
3.2 Quasi- static impact test method *20*
3.3 Fiber Pull Out Test Methodology in Fabric *23*

4 HIGH PERFORMANCE FIBER TYPES AND THEIR MODIFICATION BY PARTICULATE TO IMPROVE PERFORMANCE **29**
4.1 Stress Concentration in E glass and Kevlar *29*
4.2 Commingling fiber for wear resistance *31*
4.3 Encapsulation of fiber types to improve performance *34*
4.4 Protective system fiber types *37*
4.5 Modification of high performance yarn using GO *39*

5 HIGH STRAIN RATE FAILURE MODE **40**
5.1 PVA Fiber failure at high strain rate *40*
5.2 Failure mode related to processing *41*

6 GAP ANALYSIS OF CURRENT FIBER TYPES IN USE AND PROPOSED RESEARCH **44**

7 RESEARCH MATERIALS AND PREPARATION **46**
7.1 Yarn preparation *46*
7.2 Graphene Oxide Treatment *47*

8 QUASI-STATIC TESTING OF MECHANICAL PROPERTIES **50**
8.1 Introduction *50*
8.2 Viscoelastic materials and their behavior *51*
8.3 Static Tensile Testing (Low strain rate) *52*
8.4 Tensile Strength versus Toughness Trade-off *53*
8.5 Experimental Methodology *55*
8.6 Results and Discussion *56*
8.7 Conclusion *61*

9 DYNAMIC MODULUS TEST METHOD USING SONIC VELOCITY **62**
9.1 Introduction *62*
9.2 Basic Principles of Sonic Velocity Test Methodology *63*
9.3 Experimental Methodology *66*
9.4 Results and Discussion *67*
9.5 Conclusion *69*

10 YARN PULL OUT AND THE ROLE OF FRICTION **71**

10.1 Amonton's Law as applied to yarn friction *71*
10.2 Experimental Methodology *73*
10.3 Results and Discussion *75*
10.4 Conclusion *79*

11 HIGH STRAIN RATE FABRIC TEST USING SPLIT HOPKINSON PRESSURE BAR **80**
11.1 Introduction *80*
11.2 Hopkinson bar basic configuration *81*
11.3 Experimental Methodology *83*
11.4 SHPB Sample Set up Results and Discussion *84*
11.5 Experimental Results and Discussion *85*
11.5 Conclusion *90*

12 SUMMARY CONCLUSION **91**
12.1 Recommendations *95*

13 REFERENCES **97**

LIST OF TABLES

Table 1 List of surface modifications and the intended change to the surface of the fiber (reproduced from Coffey et al., ref 5) 8
Table 2 Type and process of surface treatment for surface modification. 11

LIST OF FIGURES

Figure 1 Typical stress strain curve 1
Figure 2 Depiction of target surface at low and high velocity (Reproduced from Bhatnagar et al Ref 4) 6
Figure 3 Typical set up of fiber pull out test method (Reproduced from Yue el al., ref 6) 12
Figure 4 Schematic showing radial, axial and hoop orientation for nanoscratch and nanoindentation. (Reproduced from: McAlister et al., ref 7) 14
Figure 5 SEM of fibrillation resulting in ploughed surface (Reproduced from: McAllister et al., ref 8) 15
Figure 6 Split Hopkinson Pressure Bar (Reproduced from REL) 18
Figure 7 Plot of specific strain energy versus strain rate showing strain rate sensitivity for Kevlar®, E-glass and PVA (Reproduced from: Wang, Y. et al., ref 9) 19
Figure 8 Quasi-static punch shear test equipment showing placement of test sample (reproduced from: Erkendirci et al., ref 10) 21
Figure 9 Energy dissipation in laminate as a function of thickness (Reproduced from Erkendirci et al., ref 10) 22
Figure 10 Graphical representation of scoured versus greige fabric velocity response curves. (Reproduced from: Nilakantan et al., ref 12) 25
Figure 11 Photo of scoured fabric with no penetration a) front of sample, b) rear of sample. (Reproduced from : Nilakantan et al., ref 12) 26
Figure 12 Image of projectile impacting fabric at a)140, b) 150, c) 170 and d) 180us showing initial separation of fibers.(Reproduced from: Grujicic et al., ref 13) 28
Figure 13 Depiction of commingling process flow and equipment. 1) Input fiber package, 2) Feed roller, 3 & 4) Guide rollers, 5) Air pressure regulator, 6) Fiber delivery roller, 7) Take up roller, 8) Commingled fiber package. (Reproduced from : Pradhan et al., ref 15) 32
Figure 14 Image of concrete slab reinforced with PVA fiber. (Reproduced from Kurrary.com/PVA-ECC) 35
Figure 15 a) Schematic of para aramid structure showing pleat structure, b) Chemical structure of Kevlar (www.wikipeidia.com) 38
Figure 16 Graphene oxide solution 39
Figure 17 PVA fiber response at different strain rates. Variation of modulus (E), maximum applied stress and failure strain, corresponding to maximum stress are plotted at several strain rates. (Reproduced from: Wang et al ., ref 21) 40
Figure 18 Effect of strain rate on tensile strength in unwoven yarn, warp and weft after weaving. (Reproduced from: Sanborn et al., ref 23) 43
Figure 19 a)KM2 Plus® yarn as received; b) PVA yarn as received 46
Figure 20 Sections of commingled yarn showing yarn bundle changes, incorporation of PVA yarn in KM2 Plus® bundle. 47
Figure 21 Schematic of typical commingled yarn showing relative dispersion of both fiber types. 47
Figure 22 Schematic of process flow for graphene oxide treatment of yarn. 48

Figure 23 GO dispersion in fiber bundle a) 2mg/ml solution treatment b) 1:10 GO dilution 48
Figure 24 SEM image of commingled KM2 Plus® & PVA with 2mg/ml GO solution treatment. 49
Figure 25 SEM image of KM2 Plus® & PVA with 1:10 dilution of 2mg/ml solution.... 49
Figure 26 Stress strain curve for a) brittle material and b) ductile material 54
Figure 27 Instron® yarn capstan grips and side view of grip curved surface. 55
Figure 28 Quasi-static stress strain curve of KM2 Plus® showing five of the ten test samples in the as received state.(Note: Offset of each specimen is added to the data for clarity & does not reflect actual prestrain) 56
Figure 29 Quasi-static stress strain curve for five of the ten "as received" specimens of PVA yarn. Note greater elongation of PVA than aramid yarn. .(Note: Offset of each specimen is added to the data for clarity & does not reflect actual prestrain) 57
Figure 30 Quasi-static stress strain curve for five typical hybrid (commingled) yarn showing initial break of aramid followed by elongation and break of PVA. .(Note: Offset of each specimen is added to the data for clarity & does not reflect actual prestrain) 57
Figure 31 Tenacity (specific strength) comparison for each yarn type. 59
Figure 32 Toughness (area under stress strain curve) for all yarn types. 61
Figure 33 Sonic velocity pathway courtesy Lawson Hemphill. 62
Figure 34 USB Oscilloscope image of waveform in KM2 Plus. Image shows voltage as a function of pulse time through material. 64
Figure 35 Longitudinal wave propagation and transverse wave propagation. (Reproduced from www.socratic.org) 65
Figure 36 Plot of sonic pulse transit time as a function of distance with linear regression curve fit. 67
Figure 37 Sonic velocity in m/sec of yarn types as tested on Lawson Hemphill LH551.68
Figure 38 Dynamic modulus calculated from sonic velocity for each yarn type. 69
Figure 39 Lawson Hemphill CTT Dynamic Friction Tester LH402 (Courtesy of Lawson Hemphill). 74
Figure 40 Yarn twist fixture showing a) yarn with no twist, b) yarn with twist and c) insert view of yarn twist. 74
Figure 41 Yarn tension profile for aramid yarn. Note spike in output tension during test. 76
Figure 42 Yarn tension profile for PVA. Note smooth and consistent profile as yarn is tested. 76
Figure 43 Yarn tension profile for aramid & PVA commingled. Sections with perturbations in tension are seen along length of profile. 77
Figure 44 Yarn tension profile for GO treated hybrid yarn. Sections with irregular output tension are smoothed. 77
Figure 45 Coefficient of friction comparison of reference yarns PVA & KM2 Plus® with commingled yarn, commingled yarn with GO treatment. 78
Figure 46 Schematic of Split Hopkinson Pressure Bar showing mechanism of projectile impact and data capture. 82
Figure 47 SHPB fabric sample with three yarns sandwiched in rubber gasket tab top and bottom to prevent sample slippage and failure at grip edge. 84

Figure 48 Initial SHPB sample fixture showing metal failure (highlighted in red) at grip sample bottom plate. 85
Figure 49 a) Second SHPB sample fixture with more robust design and increase surface area for better sample retention b) sample mounted in fixture 85
Figure 50 SHPB sample incident and transmitted pulse signal. 86
Figure 51 SHPB pulse overlay indicating shift of pulse to match slope of incident and reflected pulse signals. Slope match shown in dashed outline. 87
Figure 52 SHPB Stress strain plot of Kevlar reference, hybrid commingled yarn and GO treated hybrid yarns. 88
Figure 53 SHPB stress strain curve showing normal sample alignment by solid curves and intentional sample misalignment by dotted lines. 89
Figure 54 SHPB average modulus calculated from SHPB including intentionally misaligned samples to show effect of alignment during testing. 89
Figure 55 Yarn quasi-static modulus calculated from ASTM D 5035 tensile test method. 92
Figure 56 Comparison of modulus of yarn (sonic) and fabric (SHPB) derived from sonic velocity and SHPB tests. See Chapter 9 & 11. 92
Figure 57 SEM of aramid failure mode in a) SHPB and b) quasi-static testing showing changes in fibrillation 94
Figure 58 PVA SHPB failure modes a) fibrillation b) brittle failure. Failure in static testing had greater elongation and fibrillation. 95

1 INTRODUCTION

Protective system use has become widespread in both industrial and personal applications in the last few decades. Their purpose is to provide damage protection for equipment or personnel which may be from the impact of projectiles and or flying debris.

The field of ballistics refers to the study of projectiles and their behavior, including launch, during flight and impact. Ballistic applications require both impact and penetration resistant properties as their purpose is to slow a projectile from high velocity (~1400 ft/sec) to 0 ft/sec in a narrow time window [1]. From conservation of energy the projectile energy must be absorbed. The energy can be dissipated through rupture of the fiber or through stress waves propagated down the fiber. This ability is seen on a stress strain curve. The area under the curve is considered the toughness. It is a measure of the ability of a material to absorb energy without causing it to break.

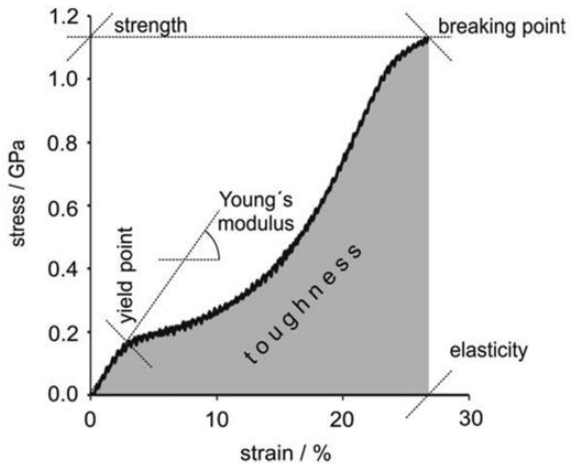

Figure 1 Typical stress strain curve

The mechanism of impact and penetration resistance is energy absorption or dissipation where the projectile may have small mass but significant energy. Many current protective systems utilize high strength, high modulus polymer fibers. These include, but are not limited to, para aramid, ultrahigh molecular weight polyethylene (UHMWPE), ultrahigh molecular weight propylene (UHMWPP) and poly(p-phenylene-2,6-benzobisoxazole (PBO). Other ballistic materials include S glass , typical composition: SiO_2, Al_2O_3, MgO, carbon and ceramics such as alumina. Based on their properties they are termed high performance fibers [4]. The ability of polymer fibers to absorb kinetic energy from projectile impact begins at the molecular level. Polymer chain bond lengths distort and elongate as they store energy on impact. Elastic modulus describes the reversible deformation of a polymer fiber as the fiber stores energy. These fibers exhibit viscoelastic behavior. Viscoelastic materials have both an elastic component, which allows the material to return to its original state after an applied load is removed, and a viscous component, which resists flow and is time dependent [2]. This viscoelastic response of the fiber to deformation includes bond interchange, chain motion, conformational change, chain coil and chain scission.

Historically materials used in personal protective systems have included paper, silk, leather, wood and metal. Changes to weaponry motivated change and improvement of protective equipment to be able to accommodate new threats. As early as 1919 there is record of patent submission for body armor. In the 1960's the discovery of new fibers ushered in the era of today's body armor. The National Institute of Justice (NIJ) proposed research into protective armor for police officers. This program, which took years to develop, resulted in a standard now called NIJ Standard 0101.06. This is the military, law enforcement and industry standard

for qualification of helmets and vests. The NIJ has also branched out to developing standards for other protective applications [3].

Currently the Department of Defense only recognizes materials as approved if they meet the NIJ standards. The various levels require testing of a completed vest, hard armor plate, helmet or other protective device by shooting the product and determining at what velocity, with the specified projectile, the product fails or stops the projectile. Other than basic testing of tensile strength of the fibers used, there are no intermediate test methods to evaluate the quality and strength properties of ballistic protective fabrics that are under development.

No simulation through Finite Element Analysis (FEA) models are used for the approval process. As a result all designs are fully developed and then shot based on NIJ or similar standards. Improvement of these systems is a continuing challenge. Current projects aim to decrease the amount of weight for any given system component so added material is not an answer. Design of the most recent enhanced combat helmet (ECH) uses a unidirectional material (all fibers are aligned in a single direction without weaving) with lower weight and higher velocity protection. Removing the out of plane condition (yarns are not linear they must go over or under each other in a woven fabric) is one means of improving the impact resistance of a system. [4] Another means to improve ballistic protection is to change to a different fiber. Fibers with a higher degree of polymer chain orientation and covalent bonding between polymer chains have also been used. Changing the surface roughness, adding chemical groups to the polymer chain to increase intrafiber friction thereby increasing energy dissipation have also been the subject of research.

1.1 Purpose of Research

The purpose of this research is to study hybridization of yarns and introduction of a frictional component to enhance ballistic performance. Furthermore, a research objective of this project was to develop additional intermediate level test methodology that may support product development and reduce the need for end item ballistic testing.

1.2 Research Questions

It is hypothesized that combining a high strength high modulus yarn with a different high strength high modulus yarn having greater elongation characteristics could reduce projectile penetration. Intercalation with GO to increase the total friction within a woven system to assist in energy dissipation may further aid in enhancing ballistic protective performance. Research questions addressed are:

- Will commingling of high performance yarns with subsequent introduction of GO into the yarn enhance strength of the fabric?
- Can high strain rate testing of hybrid yarn with and without GO treatment yield predictive algorithms of ballistic performance and reduce the need for ballistic tests?
- How does the modulus of the yarns change as a function of strain rate?
- How does sample configuration affect test methodology?
- Can the contribution of GO be evaluated by using static tensile testing if these effects may not be found at high strain rate testing?

2 LITERATURE REVIEW

2.1 Overview of Protective Systems and Current System configuration

Ballistic protective systems are a subset of the overall protective industry. They must handle high velocity impact and are used in military, police and or other governmental applications. Systems range from helmets and vests to chain saw chaps.

An extensive coverage of ballistic systems was written by a series of authors to cover protective system types, materials, modelling, standards, testing, material response, applications and new technologies. The book *Lightweight ballistic composites* [4] offered a summary of the market today. Each chapter was authored by experts in each particular area of specialization offering a useful overview, although not extremely in-depth gave information pertinent to the study of the materials.

Chapter 3 [4] focused on the response of a material to an impact event. The authors covered a combination of factors including velocity classifications, elastic and dissipative response, matrix cracking boundary conditions and projectile types. The velocity of the projectile allows categorization into two areas: low velocity and high velocity. At low velocities the system experiences a stress wave leading to failure or penetration while at higher velocities the system experiences shear or plugging. For low velocity impact there is adequate time for the energy of the projectile to be transferred to the fabric then spread throughout the system. The longitudinal stress wave stretches the yarns pulling the crimp in an orthogonal manner as a cone from the deformation is formed. As the fabric stores the energy the yarns elongate until either the projectile is stopped or there is penetration. The speed of the stress wave is

proportional to the fiber modulus divided by the density. A small component in the energy absorption is the friction from the yarns interacting between each other and between layers.

Higher velocity impacts also exhibit some of the same energy absorbing characteristics but the larger contributors are matrix cracking leading to delamination in laminate systems and shear or plugging in dry systems. The energy dissipation from the matrix is seen by formation of cracks. These are formed from normal stress, interlaminar shear stress and bending of the panel. The separation of materials, called delamination, resulting from the initial crack is a significant mechanism of energy absorption. Fibers stressed beyond their tensile strength result in breakage. For dry systems (material with no resin) the warp and weft yarns of the top layers are pushed aside by the projectile in a mode called shear plugging. The projectile is stopped as a result of the energy absorbed from yarns in compression around the projectile and friction between the yarns and the projectile.

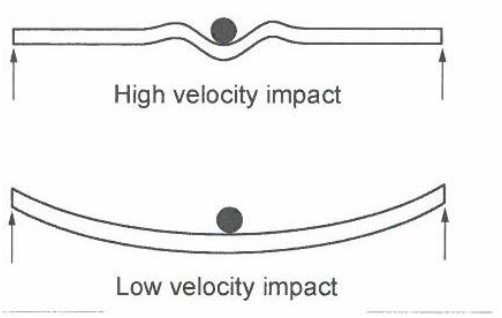

Figure 2 Depiction of target surface at low and high velocity (Reproduced from Bhatnagar et al Ref 4)

2.2 The Mechanism of Energy Absorption

2.2.1 Fiber Surface Modification

Many protective systems use composites which are a combination of high performance fibers, polymer matrices (both thermoplastic and thermoset) and/or ceramics. The fiber is called the reinforcement while the polymer or filler is called the matrix. A means to increase composite strength is to bond the fiber substrate to the matrix. The interfacial bond between the fiber and matrix is critical to allow transfer of the energy from the matrix to the fiber. The primary failure mechanisms for composites include delamination, i.e. debonding of fiber and matrix, matrix cracking and fiber pull out. For dry systems, the movement of fibers away from the projectile called windowing is of primary concern.

Study of a Twaron® polyetheramide composite was conducted by Coffey et al [5] to understand interfacial bond strength. In this study Twaron® fibers had different surface treatments to improve interfacial bonding. In Table 1 an overview of the various treatments is given.

Table 1 List of surface modifications and the intended change to the surface of the fiber (reproduced from Coffey et al., ref 5)

Surface Treatment	**Addition**
Methacryloyl chloride (MC)	Cl end group
Succinyl chloride (SC)	Cl end group
Argon gas plasma (Ar)	Surface area/roughness
Oxygen gas plasma (O)	Surface area/roughness
Nitrogen gas plasma (N)	Surface area/roughness
Ammonia gas plasma (NH_3)	Surface area/roughness/NH3 group
N-vinyl pyrrolidone UV polymerized (NVP)	Chemical bond
(Neopentyl(diallyl)oxy, tri(N-ehtylenediaminino)ethyltitanate	Ti end group
Neopentyl(diallyl)oxy, tri(m-amino)phenyl zirconate	Zr end group

The topography of aramid fibers is smooth and the polymer is chemically inert which does not promote adhesion. The purpose of surface treatment is to improve the type and degree of adhesion through chemical or mechanical bonding. This bond is integral to allow transfer of stress from the matrix to the fiber.

The addition of chloride end groups was to increase the hydrogen bond interaction between the fiber and matrix. The desired effect of the series of gas plasma treatments, although not specifically delineated by the authors, could be an increase in surface area, roughness or chemical groups (i.e. NH_3). The NVP (Table 1) was chemically bonded to the fiber using a photo polymerization technique. Surface treatments with the zirconate and titanate salts represent a class of chemicals industrially known as “coupling agents”. The fibers were

soaked in a solution of the organometallic compounds, washed and dried then treated with the resin.

Single fiber samples were prepared and tested for stress, strain and modulus on constant rate of extension (CRE) test equipment. Composite samples of each surface modified type were

made by encasing single fibers between the film. The mechanical testing of surface modified fibers did not show any significant loss of property post treatment. This included exposure of fiber to photo polymerization for NVP treatment, which had been shown in prior work as cited by the authors to degrade fiber properties.

Raman spectroscopy is a technique based on molecular vibration of bonds and is capable of detecting differences in structure geometry and bonding within molecules. The authors chose Raman spectroscopy to observe peak shift as the samples are stressed. The peak corresponding to the p-phenylene ring of the aramid fiber at 1610 cm^{-1} was monitored for changes. Deformation of the p-phenylene ring would be expected as it is a large structure in the polymer backbone. A reference value of -4 cm^{-1}/GPa for this peak shift due to stress, from published literature was used for this study.

The fibers were subjected to different levels of stress. The 'as received' fiber was the control for the comparison with the surface modified fibers. Raman spectra were able to show transfer of stress from matrix to fiber as well as detection of breaks in the fiber. Interfacial shear stress (ISS) was derived from the mapping of this stress. Visual observation of the system under stress did not show a clean fiber break. The surface of the fiber exhibited fibrillation so only "apparent" fiber breaks are identified.

The NVP treatment did improve the transfer of stress as compared to the ‘as received’ fiber. The zirconate and titanate coupling agents did not improve the stress transfer nor did the plasma treatments. Of the two treatments having a chloride end group, only the MC treatment exhibited an increase.

The use of Raman spectroscopy was successful in detecting visually determined fiber breaks and interfacial changes in the aramid thermoplastic composites as verified by peak shift and visual observation. The surface modification using NVP and MC improved the interfacial shear stress and decreased the fragment length under stress.

Raman spectroscopy was used in this study as other methods have difficulty in detecting fiber breaks. Visual observation verified there was not a true fiber break, only fibrillation in sections along the fiber axis was present. This area would no longer provide stress transfer but the fiber was still intact and could continue to carry some load. This was not discussed and the question of residual fiber strength was not addressed. While the authors did determine the effect of surface treatments, the use of plasma was not a viable option, even at the outset of the study, as noted by the authors in prior work. Plasma conditions produce a rough surface which could be useful to increase surface area, but the fiber could be degraded and plasma is a costly process for such applications.

Fiber fragment length as a function of surface treatment was shown to increase with the NVP and MC, but since this was only visually confirmed but not actually measured length more study could be performed to determine the degree of fibrillation.

The surface of the fiber is important for bonding in a composite system. Yue and Padmanabhan studied the surface morphology of solvent treated fibers to understand the

interfacial properties in an epoxy matrix [6]. Their study found a means to increase the interfacial strength from 39MPa of untreated fibers to 63MPa for a chemically treated fiber. The authors found that many prior studies focused on adhesion of the fiber in a composite but a change to the fiber surface morphology and chemistry had not been simultaneously studied. The authors studied Kevlar® 29 fiber and modified the surface to correlate properties before and after the treatment to the surface chemistry and fiber morphology. The three types of treatment are listed in Table 2.

Table 2 Type and process of surface treatment for surface modification.

Step 1	Step 2	Step 3	Step 4
Acetic Anhydride 1min	Rinse w/distilled H_2O		Oven dry, Low vacuum 5 hours
Acetic Anhydride 1min	Methanol wash 3 min	Rinse w/distilled H_2O	Oven dry, Low vacuum 5 hours
Acetic Anhydride 1 min	Methanol wash 10 min	Rinse w/distilled H_2O	Oven dry, Low vacuum 5 hours

Scanning Electron Microscopy (SEM) images of the fibers treated with acetic anhydride only displayed surface blisters, acetic anhydride plus methanol for three minutes displayed striation and acetic anhydride plus methanol for ten minutes exhibited areas of exposed core. Obtaining good wet out of the surface (surface energy of matrix vs that of polymer) is critical for sufficient bonding of the matrix to the substrate. X-ray photoelectron spectroscopy (XPS) analysis found the surface of the fiber treated with acetic anhydride only to have the highest surface oxygen content followed by the methanol treated samples. Prior

experimental evidence reported the oxygen content is key to wetting and bonding with resin systems. All of the solvent treated fibers had higher surface oxygen content than the untreated fiber. The chemical change resulting in increased surface oxygen content and surface morphology change also influences the interfacial bond. Atomic Force Microscopy (AFM) analysis of the surface of the treated samples confirms the roughness of the surface. The surface roughness could be a source of the increased frictional stress and interfacial shear strength as seen in the samples.

The fiber pull out test method was used on multiple fibers to determine the interfacial frictional stress τ_f and the interfacial shear strength τ_i . This test method places the sample embedded in the resin in a fixture. Fibers are then pulled out and the load calculated to achieve break or dislodge the fiber(s) from the matrix. Both the acetic anhydride only and acetic anhydride plus 3 minute methanol wash sample had higher τ_f and τ_i pointing to the combination of improved surface oxygen content and microroughness of the surface increasing the interfacial bonding.

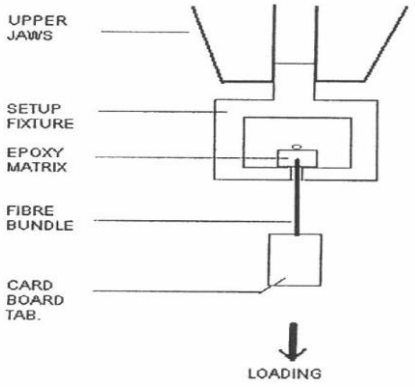

Figure 3 Typical set up of fiber pull out test method (Reproduced from Yue el al., ref 6)

Significant improvement in interfacial frictional stress was seen in the acetic anhydride treated sample only. More improvement in the interfacial shear strength was observed in the acetic anhydride plus 3 minute methanol wash. Yue et al established a means of improving interfacial shear of composite structures of p-aramid and epoxy by correlating the surface chemistry, i.e. surface oxygen content, and the fiber morphology to interfacial characteristics of the composite.

The authors utilized an array of techniques using the results from one test to confirm findings in another. This paper correlated the hypothesis with data but missing from the data was information on the epoxy they used. There are many types of epoxy with different functional side groups, the type would have been useful for comparison studies. Further studies proposed are to evaluate the surface hydrogen and how the etched surface changes as the polymer chain linkages are broken or reformed.

2.2.2 Utilization of nanoparticles for nanoindentation and nanoscratch

Fabric performance has been shown to be limited by spreading apart of the yarns as a projectile penetrates the fabric. The amount of this separation can be modified by an increase in the friction within the fiber. The addition of nanoparticles has also been shown to improve the fabric performance as they increase this friction component within the fiber.

In the study by McAllister, Gillespie and VanLandingham, their objective was to understand the relationship between surface scratch and indentations to the interfiber friction of a woven Kevlar® fabric with nanoparticles incorporated [7]. The size of the nanoscratch made is approximately the same as the microstructure of the Kevlar® 49 and KM2 fibers that were compared in this test. In a previous work the authors had defined a “critical contact size.”

The critical contact size being the point where the "local fiber response is no longer sensitive to the microfibril heterogeneity" [8]. Initial nanoindentation in the center of the fiber as well as the radial and axial orientations of the surface established the contact size sensitivity (in the range of this study). A nanoparticle assumed to be spherical would impart a scratch on the fiber surface in relation to its contact depth. To simulate this, different angles between the scratch probe and surface (attack angle) and different probe geometries were used.

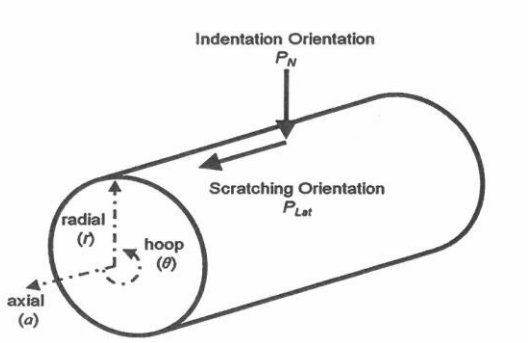

Figure 4 Schematic showing radial, axial and hoop orientation for nanoscratch and nanoindentation. (Reproduced from: McAlister et al., ref 7)

To prevent movement of the fiber during testing polystyrene (PS) was used to attach the fiber to a glass plate. Removal of the PS was accomplished by an initial low depth scratch.

Three modes of deformation were observed and identified as "ironing, fibrillation and mixed mode. The fibrillation and associated build-up of broken polymer in front of the probe were a typical response during the scratch. As this build-up occurred the forces in the normal and lateral direction increased over the distance of the scratch. The apparent friction increased in relation to the scratch distance confirming that the nanoparticles did increase the interfiber friction of the fabric. The scratch maps and AFM images generated for Kevlar® 49 and KM2

show Kevlar® 49 resisting fibrillation initially better than the KM2 fiber at different attack angles and degree of friction. The difference for KM2 fiber was noted in a previous study showing this fiber as having a shell with reduced stiffness. Both fiber types maintained their tensile strength post nanoindentation to larger depths than the proposed infused nanoparticles. McAllister and coworkers were able to show KM2 resisted the start of fibrillation at higher attack angles than K49. Indentation testing showed the fibers kept their tensile strength, even with deeper indentation, which could permit property improvement for energy dissipation using nanoparticles.

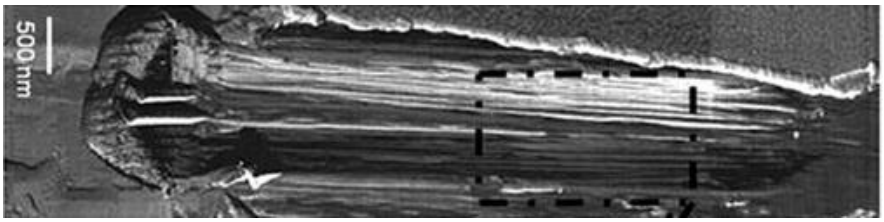

Figure 5 SEM of fibrillation resulting in ploughed surface (Reproduced from: McAllister et al., ref 8)

The sample frequencies of the study included over 40 fibers permitting meaningful testing to include fiber variation. The use of PS to attach the fiber was critical to obtaining useful information via AFM. The concern with the film is that it could possibly contribute to the actual test data. This was addressed by their film removal procedure. The procedure was substantiated by images of the removed film build up after the low depth scratch. However, later mention of the film and interaction of the nanoindentation test with the edge of the film indicated it still could possibly be present in the test data. The authors felt the presence of the film would not significantly change the data as the majority of the exposed surface was film

free. They were able to show that nanoparticles could improve properties through fiber particle interactions but only a single study was referenced so there was no ability to note optimum level, size or geometry of particle incorporation.

3 BALLISTIC PROPERTY TEST METHODOLOGY

Testing of the ballistic properties of vests and helmets standards around the world have been developed such a NIJ, ASTM, Military and Underwriters laboratory (UL). The type, level and test methodology are listed in the standards. To achieve certification to a specific threat level sample "ballistic packs" must be shot. Ballistic limits are identified in terms of projectile velocity. The term V_x where V, the projectile velocity at any given x, is the probability the fabric will experience penetration. The V_{50}, which is the velocity at which half of the projectiles did not penetrate and half did penetrate, and the range of velocities are reported for submission to the customer.

3.1 High Strain Rate Testing with Split Hopkinson Pressure Bar

Determining mechanical properties of protective systems and their components is accomplished using a variety of test equipment. The American Society for Testing & Materials (ASTM) and other recognized methods are in place to standardize testing between labs. One method used for testing at high strain rates is a Split Hopkinson Test Bar. The SHPB is capable of testing materials at high strain rates of approximately 1000/s. The equipment consists of 2 large steel bars mounted on a frame. Samples are loaded between the incident bar and the transmission bar. A bar moved by compressed air, termed a striker, strikes the incident bar which causes a stress wave that propagates through the incident bar. As it reaches the samples it splits into 2 smaller waves. Part of the wave is reflected back into the incident bar and the other travels through the sample into the transmission bar. Strain gauges installed on the incident and transmission bars record the strain caused by the stress

wave. The reflected pulse is used to calculate the strain and the pulse that continues through the samples is used to calculate stress.

Figure 6 Split Hopkinson Pressure Bar (Reproduced from REL)

Time dependent response of high performance fibers was the subject of research by Wang et al [9]. In protective systems, ballistic properties of the composite are a function of the ability of the fiber to bear the applied load. Understanding the response of the fiber under ballistic conditions, which involve high velocity is critical for the application and design of these systems.

SHPB impact testing was performed on E-glass, an alumino-borosilicate glass with less than 1% w/w alkali oxides, Kevlar®49 and polyvinylalcohol (PVA) fibers at different strain rates. Stress strain curves of the fibers show that all fibers exhibit a correlation to the rate of strain. The PVA fiber only exhibited an increase in maximum stress applied to the fiber, σ_{max} and the strain resulting from the maximum applied stress, ε_m , but the modulus had no significant

change. High strain rates involve the elastic component of the fiber properties while low strain rates involve the viscous component. The absorption of energy by the fibers is through the elastic component. The authors define the area under the stress strain curve as the tensile strain energy. To compare tensile strain differences between the fibers they define a specific strain energy, U_c for a given strain rate as follows:

$$U_c = \tfrac{1}{2}\ \sigma_{max}\ \varepsilon_{m/}\ \rho \qquad (1)$$

where ρ = fiber density.

Plotting U_c as a function of the log of strain rate clearly shows the Kevlar®49 having the highest capacity in ability to change molecular configuration under tensile strain. The Kevlar® fiber consistently absorbs energy with much less elongation than the E-glass and PVA (Figure 7).

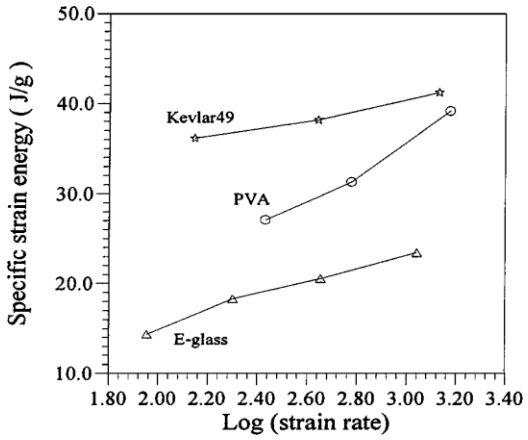

Figure 7 Plot of specific strain energy versus strain rate showing strain rate sensitivity for Kevlar®, E-glass and PVA (Reproduced from: Wang, Y. et al., ref 9)

Each fiber exhibited strain rate dependence with E-glass and PVA having significantly greater rate coefficients than Kevlar® with the exception of the elastic modulus.

Observation of the broken fiber ends via SEM show the failure modes for each fiber. SEM of the E-glass fiber shows a sharp break in a brittle manner. The PVA had two types of fiber break one was brittle having a clean fractured end and the other had fibrils resembling that of Kevlar® indicative of a similar mode of failure. The authors indicate the mode of failure is the reason for the higher mechanical properties for Kevlar® and PVA fibers.

Kevlar®49, PVA and E-glass all show a correlation to strain rate. The Kevlar®49 exhibited lower strain rate sensitivity and has better performance than PVA or E-glass in a ballistic environment. The non-brittle failure mode of PVA along with the observed high U_c at a high strain rate would place PVA in a similar category as Kevlar®49. No minimum requirement or reference standard was given in the paper. E-glass is known for brittle failure, but has been shown to perform better in combination with other fibers.

3.2 Quasi- static impact test method

The goal to optimize energy dissipation and reduce weight in ballistic composites is part of on- going work in industry. A study to evaluate the quasi-static penetration resistance performance of a high density polyethylene (HDPE) and Kevlar (aramid) composites was the focus of Erkendirci and Haque [10].

Quasi-static-punch shear test (QS-PST) is a method to determine degree of projectile penetration. The author's state that compared to other industry standard tests, i.e. Charpy, Izod (high strain rate impact test), etc.., QS-PST is an easier method providing data from

both the damaged and undamaged sections of the sample. QS-PST tests the samples at very low strain rates. A custom steel fixture with punch and punch guide is fabricated allowing different sample sizes to be tested. Support spans are used behind the samples and can have different diameters for each specimen size. Testing at various ratios of support span diameter and punch head diameter provided test data for the shear and bending component of the composite.

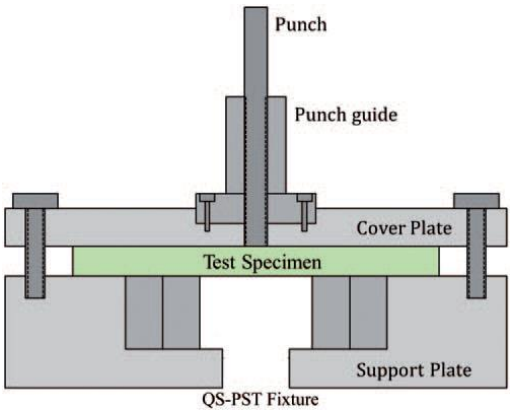

Figure 8 Quasi-static punch shear test equipment showing placement of test sample (reproduced from: Erkendirci et al., ref 10)

The authors were conducting follow up to their prior research using the QS-PST method in work to develop measureable quasi-static penetration energy. A series of composites consisting of 4, 8 and 12 layers of a plain weave aramid and HDPE film were produced using a hot compression mold.

Penetration energies of the composite with different thicknesses were determined by analyzing the load (force per unit area of laminate) displacement data. The area under the stress strain curve is the work done as energy dissipation.

The aramid HDPE composites exhibited initial non-linear displacement followed by a linear portion which continued to maximum force. The authors assumed there was no fiber damage up to maximum force. They stated the major influencing factor for the changes in the laminate are from “non-linear membrane tension shear” around the punch head. The mode of failure is seen as elastic deformation followed immediately by fiber fracture near the maximum load as seen by the large decrease in resistance force. The 12 layer composites, as expected, had the highest maximum force required. Figure 9 shows the function of thickness in energy dissipation.

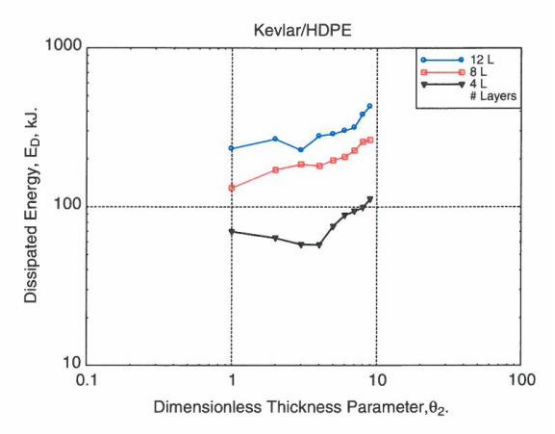

Figure 9 Energy dissipation in laminate as a function of thickness (Reproduced from Erkendirci et al., ref 10)

Comparison of the 4, 8, and 12 layer composites, tested at the same SPR, show a failure mode of fiber pull out and not brittle fracture. The authors state the ‘”matrix crack mode is naturally absent in aramid HDPE” as the matrix responds in an elastic deformation manner up to the maximum load. My concern with this statement is as the matrix elongates it will pull away from the reinforcing fiber as the bond is mechanical and weak. This is matrix

cracking. The amount of cracking may not be well seen and delamination may be limited, but failure of the interface will occur. For optimum bonding the thermoplastic or thermoset must thoroughly flow and adhere to the surface to be bonded. The surface energy of the fiber should be greater than the surface energy of the resin. This degree of bonding is termed wet out. Wet out can be measured by the contact angle of a bead of the resin on the fiber surface. The smaller the contact angle the more the surface wets out and vice versa. Aramid surfaces are smooth and relatively inert not promoting adhesion. Their hypothesis of limited wet out by the HDPE of the aramid is accepted. This does not completely support the failure mode of fiber pull out. Fiber pull out occurs as the energy is transferred to the fiber and the interface fails. Assuming no fiber damage up to maximum force was not substantiated by any data presented.

Plotting the area under the force displacement curve as a function of thickness shows clear delineation of the fiber capacity to accommodate impact. The 12 layer composite showed the highest energy dissipated, the 4 layer the lowest, indicating dependency on thickness which has been well developed in other literature.

3.3 Fiber Pull Out Test Methodology in Fabric

Fiber pull out is a test performed on woven protective systems. There is no standardized test method so Nilakantan et al [12] modified the industry type of testing and used the results for their experimentation. Testing of samples has the sample encapsulated in the matrix with both ends exposed. The force required to pull out the fiber is recorded as a function of length encapsulated and the interfacial shear strength is calculated [11]. In this case only the woven fabric was used and placed in a custom fixture to simulate ballistic vests with no matrix.

Experimentation of greige (loom state) and scoured (hot water or solvent wash) plain weave Kevlar KM2 fabric to determine the probabilistic velocity response (PVR) was performed. The mode of failure during impact was studied using single ply of 180 gsm fabric mounted in a custom fixture to permit principal yarns to respond in an unclamped state. On impact yarn can fail under tensile strain, in shear as the energy of the high velocity projectile cuts the fiber or from movement of individual yarns away from the projectile "windowing" allowing the projectile to penetrate the fabric. Windowing occurs as the yarns slide across each other and ultimately are pulled out creating a hole. Single yarn pull out testing was also performed to validate the inherent variation of the yarn. Pull out speeds of 50 mm/min and 500 mm/min were applied to each specimen. No significant difference was observed between the greige and scoured fabric. The warp pull out load was found to be higher than the fill pull out load. The pull out load was found to be rate dependent with greater loads required at low velocity.

For ballistic testing samples were placed in a custom equilateral octagon (EO). The design has corner grips for the samples allowing the principal yarns to move unclamped. Sample orientation at the edge of the EO was noted for verification of any slippage during testing. Impact tests consist of a gas gun firing the steel projectile with measurement of velocity by chronograph and residual velocity captured with light screens behind the target.

The PVR curve generated for scoured fabric shows higher impact properties than the greige at low velocity (V_1). The greige fabric at higher velocities had better impact properties. Comparison of the coefficient of variation for greige versus scoured show a threefold difference indicative of greater variability for the greige fabric.

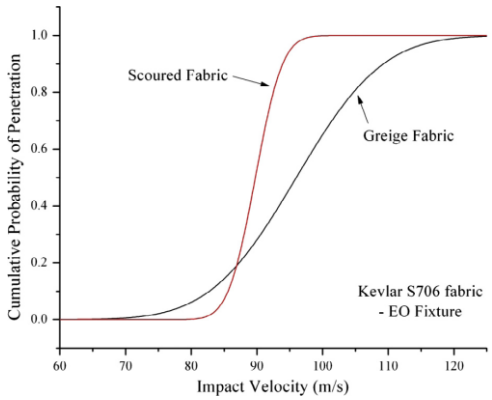

Figure 10 Graphical representation of scoured versus greige fabric velocity response curves. (Reproduced from: Nilakantan et al., ref 12)

Observation of each sample for pull out and penetration found scoured fabric had greater number of penetrations. Greige fabric had few instances of penetration. In cases where the fabric contained the projectile, the yarn is flat. It was postulated under compression by the projectile the filaments open up increasing the actual width of the yarn helping contain the projectile.

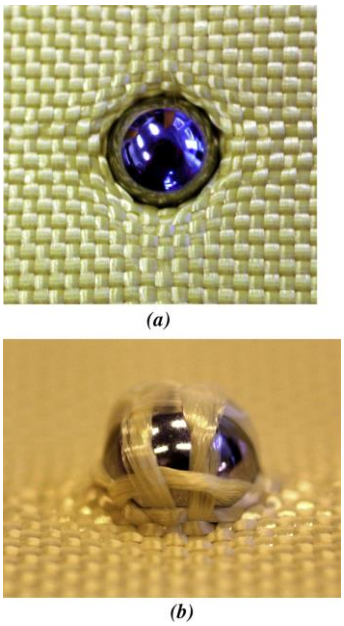

Figure 11 Photo of scoured fabric with no penetration a) front of sample, b) rear of sample. (Reproduced from : Nilakantan et al., ref 12)

For all ballistic samples with penetration the failure mode was windowing with no complete yarn failure of principal yarns. The EO fixture allowing principal yarns to move freely would permit these yarns to pull out rather than rupture on impact. The study found no yarn strength failure yet there was windowing. The freedom of principal yarns to move in the EO fixture does not necessarily represent real world applications.

The number and length of principal yarns pulled out varied. The study did not measure the coefficient of friction but did assume friction as the largest influencing factor for energy dissipation as the frictional contribution from greige versus scoured from yarn sliding varied from sample to sample. Greige fabric had a higher degree of yarn pull out compared to scoured fabric which follows the PVR curves. To explain the difference the authors state the windowing effect is greater when the projectile directly impacts at the intersection of the

warp and fill fiber or between yarns. They point to neat holes at the impact site that had yarn push out. They indicate that scoured fabric had larger interstices versus greige which would explain the difference in values. This could result in more yarns being pushed aside leading to penetration. A second theory was of frictional interaction between projectile surface and yarn filaments of the different fabric types. The back of the sample after impacts shows frictional sliding over the projectile surface. A third theory was of the friction within each yarn contributing to the mechanics of the yarn separating.

The study was able to show a relationship of frictional components to impact response at low velocities. They found greige fabric had higher V_{50} values and scoured fabric performed better at low velocities. To improve performance at higher velocities inter-yarn friction would require modification.

While the frictional components are important, typical protective systems use a water repellant after scour or use scoured fabric in a resin matrix. This then limits the data presented. The contribution of spin finish (coating on aramid yarn as protection in processing) while mentioned was not addressed in their theories for frictional sliding and could add texture to the fiber surface. The EO fixture is new and attempts to mimic large sample behavior but the size of the fixture and free principal yarns do not mimic large samples or closed systems well as the fixture allows freedom of movement of some yarns which is not present in actual protective systems. .

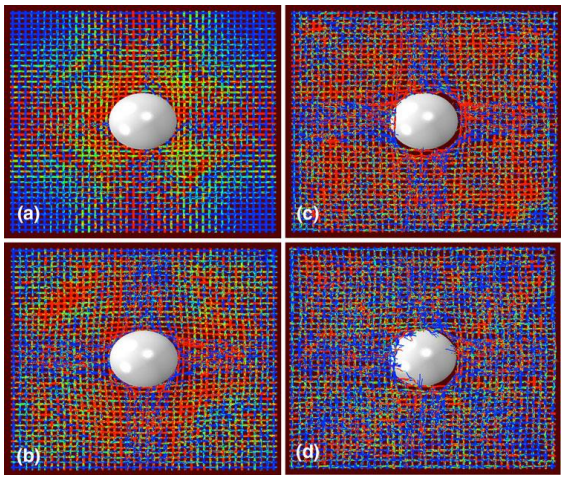

Figure 12 Image of projectile impacting fabric at a)140, b) 150, c) 170 and d) 180us showing initial separation of fibers.(Reproduced from: Grujicic et al., ref 13)

4 HIGH PERFORMANCE FIBER TYPES AND THEIR MODIFICATION BY PARTICULATE TO IMPROVE PERFORMANCE

4.1 Stress Concentration in E glass and Kevlar

Studies of the interactions in the different combinations of reinforcement (E glass, aramid, S-glass, carbon, etc…) and resin (epoxy, polyester, phenolic, thermoplastic) is often used to characterize system reliability. Zhou et al conducted a study of the stress concentration profiles of Kevlar® in hybrid composites [14]. The authors tested single fiber composites to estimate stress distribution as the composite is strained. Typical composites have a weak mechanical bond with the matrix unless a surface finish (chemical treatment applied to fiber for protection or bonding) is applied to the fiber that can increase the bond to both the fiber and the matrix. As the fiber breaks stress is transmitted to the surrounding area. The mechanism of stress transfer involves both the fiber matrix interface and interfiber and/ or intrafiber interactions. Fiber reinforcement will fracture upon impact. Stress from the impact is dissipated by the fiber. Along the area of impact the stress builds leading to regions of stress concentration which in turn eventually lead to failure of the fiber. As the authors found, very little experimental work has been done to validate the stress concentration from a lack of established measurement methods.

E-glass fibers typically have a PVA starch solution applied as they form to protect them. This is called sizing. If this is not applied or is removed the fiber is considered unsized or desized. Unsized and sized E-glass fibers along with Kevlar® were used in testing. The E-glass fibers were approximately 12 μm in diameter. Fibers were coated with an epoxy resin. The E-glass was highly prestressed prior to addition of the resin and the Kevlar® was prestressed at a lower weight. A series of interfiber distances (μm) were tested to determine the role distance

plays in the interaction of the stress concentration factors (SCF). The hybrid composite was tested at a strain rate of 0.2 -0.4 μm/s. Microraman spectroscopy captured the spectra of the Kevlar® peak vibrations at 1287, 1328 and 1611 cm^{-1}. As the fiber was stressed a peak shift was observed to a lower wavenumber. The shift of the 1611 cm^{-1} peak was monitored with each break in the E-glass fiber. As the fiber breaks and transfers stress to surrounding areas the fiber nearest the broken fiber is the first to experience the stress transfer. Redistribution of stress is affected by the distance to the nearest fiber and by the bond to the matrix. The SCF is defined as the ratio of local to applied stress. The stress and strain associated with each of the multiple breaks in the E-glass fiber was logged until no failure of the matrix was observed. The authors identified full debonding if they observed "deep dark and grey lines" and partial debonding if the lines were "thin and faint". They observed no loss of interfacial bond in the sized E-glass samples.

Debond length along the fiber was used to calculate the stress concentration factor, (*K)* by the equation

$$K = 1 + \left| \nu_x - \nu_\infty \right| / \left| \nu_\infty - \nu_0 \right| \qquad (2)$$

Where :
ν_x = Raman peak wavenumber (cm^{-1}) at the cross section of the fiber break
ν_∞ = Raman peak wavenumber (cm^{-1}) at the far-field position away from the break cross section
ν_0 = Raman peak wavenumber (cm^{-1}) with no applied strain

For most cases the experimental values in this study calculated higher SCF values than theoretical values by a factor of 1.5X.

In comparing the sized versus unsized fiber the Sized E-glass had a higher SCF than unsized. Sized E-glass exhibited clean matrix breaks accompanied by some crack formation and unsized exhibited interfacial failure. Debond lengths were shorter in sized fiber samples than the unsized. The improvement in bond strength is well accepted in literature as the sizing, which in this case is silane, provides a much stronger mechanical bond to the glass than the unsized. The authors did not clarify if the sized fiber had the manufacturer's size only, nor did they indicate if the fiber had any twist, which is a designation of if and how much the fiber has been twisted on its axis, this could alter the difference in the stress concentration factor.

The model proposed is only valid where the matrix does not fail, as the authors only evaluated the portion of the stress strain curve after prestressing the fibers, and therefore has limited use.

4.2 Commingling fiber for wear resistance

Commingling of different fibers will provide a more homogenous fiber as the two types have a uniform distribution profile. The influence of the weight fraction of aramid and polypropylene (PP) composites was studied by Pradhan et al [15]. Unidirectional high performance fiber reinforced polymers (FRP) have application in aircraft, pipeline and recreational equipment. The reduced weight and wear resistant properties are key factors in their use. Aramid fibers have been shown to increase wear resistance in various products. The addition of thermoplastics to FRPs is utilized for the impact properties and toughness. Many thermoplastics have a high viscosity which increases process time. Combining the matrix fiber with the reinforcing fiber yields a solution to this problem. The thermoplastic

fiber is in direct contact with the reinforcing fiber allowing a direct path during flow to encapsulate and or adhere the reinforcing fiber. Mechanical properties related to fatigue, impact and deformation have been studied but there are few studies on tribological performance. Pradhan et al set out to determine the influence of reinforcing fiber weight fraction in a commingled fiber. Evaluation of property improvement from incorporation of a reinforcing fiber would need to include total amount of fiber added, type, fiber orientation and ability to increase adhesion to the matrix.

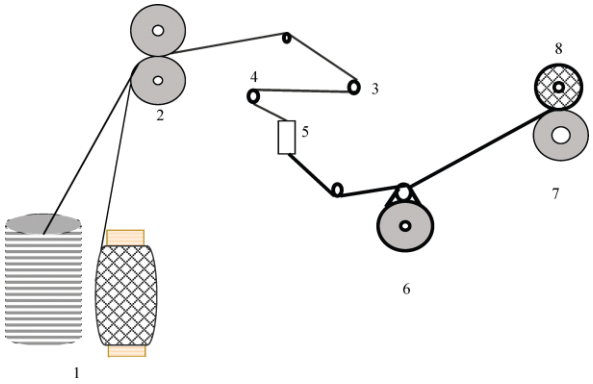

Figure 13 Depiction of commingling process flow and equipment. 1) Input fiber package, 2) Feed roller, 3 & 4) Guide rollers, 5) Air pressure regulator, 6) Fiber delivery roller, 7) Take up roller, 8) Commingled fiber package. (Reproduced from : Pradhan et al., ref 15)

Four different weight fraction composites (0, 18,24 & 29%) were made and studied. [15] The aramid fiber was Kevlar®29 with the PP a multifilament yarn. The commingled yarn was wound on a frame in one direction, then placed in a mold for consolidation.

Abrasion wear studies with loads of 20, 30, and 40 N were conducted on a Universal wear tester. Each test was repeated and the average value of weight loss used for calculation of wear rate. Samples were tested at 0^0 and 90^0 orientation.

Abrasion studies show as the aramid weight fraction increased the wear area decreased. When the composite was abraded perpendicular to the fiber orientation there was less wear. In the perpendicular orientation the increase in aramid weight fraction followed the decrease in wear rate. However, in the parallel orientation there was lower wear resistance. The authors noted fibers were peeling out of the composite in this orientation producing higher wear rates. Overall, the aramid fibers with orientation perpendicular to abrasion increased the wear resistance with orientation as the factor with greater influence.

Erosive wear testing was performed per ASTM G76 in an air jet erosion rig. Weight loss samples were used to calculate erosion loss. Tensile testing per ASTM D3039 was performed on multiple samples. The modulus and specific strength increased with the increase in percentage of aramid fiber. However, as the percentage of aramid increase there was less strain to break.

Erosion studies show the composites with more aramid had a three-fold improvement. Fibrillation of the aramid, during erosion, along with the capacity of the aramid to resist wear, were cited as the reasons for improvement. The erosion wear rate and abrasion wear rate were approximately the same with the increase in aramid fiber weight fraction.

Commingled PP yarns with varying aramid weight fraction improved the tensile, abrasion and erosion wear rates for unidirectional composites. Orientation of the fiber was critical to

optimization of the wear and abrasion properties. Commingled fibers provided combined properties with less cost and reduced process time.

4.3 Encapsulation of fiber types to improve performance

The addition of other materials including steel, carbon and polymeric fibers has been shown in studies to improve penetration resistance. Mechanical properties including ductility, load carrying capacity, flexural strength and crack development were used in a study by Almusallam et al to evaluate the addition of such materials and the changes to impact properties [16]. A series of reinforced concrete (RC) slabs were cast with different volume fractions of hooked end steel, polypropylene Type-2 (PP2) and Kevlar®. The prepared specimens of hybrid fiber reinforced concrete (HFRC) for each combination used steel fiber. The steel fiber is the largest contributor to improvements while the other materials were added to change properties such as toughness, micro-cracking and penetration depth. Slabs with single or multiple fiber combinations were impact tested with an air gun system. An 8 mm steel projectile with a hemispherical nose was used for the study.

Several criteria and measurements were used to evaluate performance. Damage levels were rated according to the levels set by Dancygier et al [17]. The assignment of damage from lowest to highest (rated 1-6) was obtained from the rear panel of each specimen. Physical measurements of the damage were from penetration depth and crater size. To differentiate standard concrete and the HFRC panels in compression, simulating the rear of the panel at penetration, the authors also conducted a split tensile test. The split tensile test per ASTM C496 requires a cylindrical sample be prepared with the experimental raw materials, kept in water during cure cycle then tested by placing the sample in a horizontal position to

determine the compression load for failure. The HFRC samples had a higher average split tensile strength as compared to the standard concrete. This explains the lower amount of front and rear panel damage.

The reported experimental ballistic limit was taken from the average of the velocities with and without perforation of the test panel. Hooked end steel panels exhibited the highest ballistic limit. Data from the study shows this was directly related to the presence of the hooked end steel fibers. Test panels with PP2 fibers had similar results to hooked end steel samples but also had significant abatement of concrete fragments. The addition of Kevlar® fibers, with a lower amount of hooked end steel fibers was weaker on impact but also had better constraint of the concrete fragments. Samples with all three fibers increased the impact resistance with lower penetration depths. The test values show the panels with all three fibers performed better than panels with only two types of fiber as observed from damage levels and crater dimensions. Synthetic fiber addition localized the damage and only minor cracks were evident.

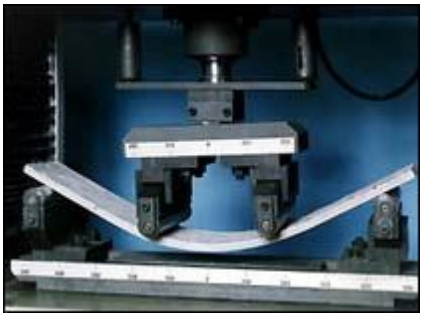

Figure 14 Image of concrete slab reinforced with PVA fiber. (Reproduced from Kurrary.com/PVA-ECC)

Prediction of penetration depth was a focus in earlier work by the authors and building on this work they modified the equations for the fiber types used in the current work to compare to experimental observation. Comparison of predicted versus experimental values show a +/- 10% difference, which is considered within accepted error levels with the limited and unknown portions of the model parameters. The experimental data clearly shows the volume fraction of hooked end steel had the highest contribution to reduction in penetration depth and PP2 had the lowest. The conclusion was that the diameter of the PP2 fiber as compared to the dimensions and shape of the hooked end steel did not increase its contribution as much. The Kevlar® yarn used had a low profile and test values did not show their inherent higher tensile and modulus values translate to an increase in impact properties. As the slab was weaker the authors postulate the geometrical properties of the yarn are more influencing than the material properties in response to impact resistance of HFRC.

The problem noted in the study is the inability to collect experimental data for RC ballistic events. Therefore, the authors identified a range where the hypothetical ballistic limits would be and plotted the average of minimum and maximum velocity with and without perforation. The notation of good was placed for each predicted value if it was within +/- 10% error and no good if greater. The conclusion that hybrid yarns decrease the dimensions of the damage to a RC slab and mitigate crack development was shown. However, the proposal that the geometry of the yarn had any effect was not substantiated in the discussion. The volume of such a fiber as compared to the other fibers did not necessarily point to the geometry of the fiber. The length and orientation of the fiber could also have made a difference. Possible mathematical models based on volume fraction and analysis of the failure zone could point to the true failure mode.

4.4 Protective system fiber types

Aromatic polyamides are known as para-aramids (p-aramid) as well as poly para-phenylene terephthalamide) or PPTA. Their use in protective equipment and industry has saved lives and improved the performance of several products. They are a class of liquid crystal polymers. In solution they flow like a liquid but the molecules are oriented in a crystal like structure. P-aramids were first created in 1965 by Stephanie Kwolek and Herbert Blades of DuPont [18]. They are produced by a low temperature condensation reaction of an amine and an acid chloride. The polymer produced is filtered, washed and dissolved in concentrated sulfuric acid then extruded through spinnerets to form the fiber. After a wet spin process the polymer is coagulated in sulfuric acid followed by washing and neutralization. To produce different denier or different moduli fibers, the fiber is taken through different heat treatments and tension processes. The manufacturing process is critically important in developing the orientation of the crystalline regions of the polymer. The repetitive sequence of the molecular backbone containing the aromatic group, benzene, with a para orientation gives rise to its rod like structure. The overall morphology has been the subject of many studies [36,37] and its structure is described as polymer chains parallel (Fig 1b) to each other arranged in a radial pattern with hydrogen bonds between the chains. The fibers consist of sheets with a regular pleat along the length axis. (Fig 16a)

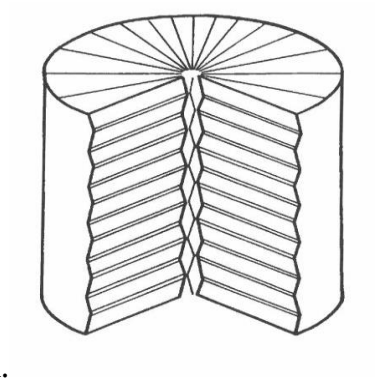

a.

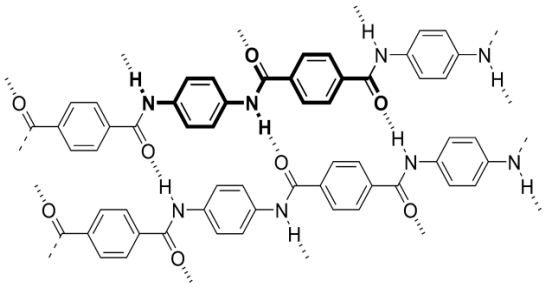

b.

Figure 15 a) Schematic of para aramid structure showing pleat structure, b) Chemical structure of Kevlar (www.wikipeidia.com)

KM2 Plus® yarn used in this study is identified as a fiber with high toughness and tenacity having a finer denier than the KM2. This particular aramid was chosen as it is a good base material in protective systems and is already in use in several products. (www.dupont.com/products)

High strength, high modulus polyvinyl alcohol fiber (PVA) has been used as reinforcement in rubber, plastic and cementitious products for non-asbestos applications [19]. New applications using PVA in military shelters or other composites for penetration resistance continues to grow. Incorporation of high strength, high modulus PVA in impact applications may improve penetration resistance.

The fiber is produced by gel-wet spinning method. The input PVA has a degree of polymerization of approximately 1700 molecular weight. The input spin solution is comprised of the PVA with alkali and boric acid added along with other solvents. PVA fibers entangle easily and efforts are made in processing to reduce this effect. The process is

conducted in a closed system allowing for reclamation of solvents. The PVA undergoes spinning and drying. After drying, the fiber goes through a drawing process. The drawing process aligns the molecular chains producing high strength with the high degree of orientation of the chain [20]. The T_g of the produced PVA is 85^0C.

4.5 Modification of high performance yarn using GO

Graphene oxide is a form of graphene that has been oxidized by reaction of graphite with a strong oxidizing agent ($KMnO_4$) in an acid media. During the reaction the suspension is kept at a low temperature. The final mixture is diluted and filtered through dialysis media to remove impurities. Having oxygen groups, graphene oxide is hydrophilic and therefore easily dissolved in water. Particulate size ranges from micron to nanometer.

Utilization of particles infused into high strength fibers have been shown to increase the friction within a fiber. The particles move, scratch and gouge the fiber surface resulting in an increase in energy dissipation related to the energy to move the particles. Graphene oxide particles may be used in such applications.

Figure 16 Graphene oxide solution

5 HIGH STRAIN RATE FAILURE MODE

5.1 PVA Fiber failure at high strain rate

Wang et al [21] conducted a study of PVA fiber to evaluate the effect of high strain rate in military shelters as shock abatement. The energy dissipation by the fiber can be used in calculation for the design of the shelter. The researchers used Split Hopkinson Tensile Bar to test the effect of strain rate and report the distribution of statistical variance in the fiber. The strain energy is recorded by strain gauges which then are used to calculate the stress and strain in the samples with respect to time.

Three different stain rates used were 270/s, 600/s and 1500/s. PVA shows a dependence on strain rate with an increase in stress (σ_{max}), and strain (ε_m) with an increase in strain rate ($\dot{\varepsilon}$).

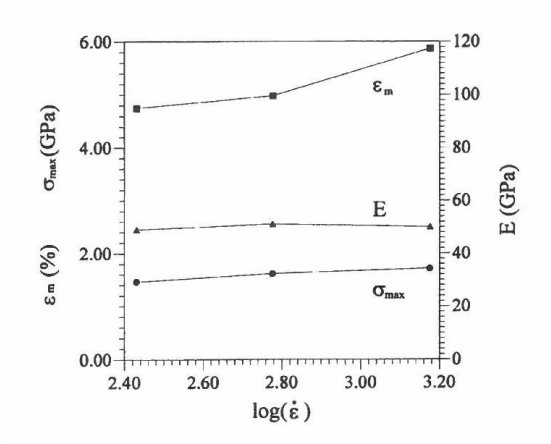

Figure 17 PVA fiber response at different strain rates. Variation of modulus (E), maximum applied stress and failure strain, corresponding to maximum stress are plotted at several strain rates. (Reproduced from: Wang et al ., ref 21)

The modulus E has no significant change. Analysis of the PVA fiber after testing shows two different failure modes. The first mode had a sharp break, similar to aramid fiber as it fibrillates. The second mode has a flat splayed end. The authors linked the modes of failure to different types of fiber defects which would limit the strength of the fiber. A four parameter Weibull distribution was used to evaluate the statistical spread of the fiber strength. Parameters for the Weibull distribution are m_1 and m_2 for the shape and σ_{01} and σ_{02} for the scale, as related to the two different defect types. Weibull plots show 2 regions which the authors indicate represent the two different defect types. Using the Weibull parameters the simulated stress/strain curve agrees with the data from the experiment.

The authors presented the strain rate dependence of the PVA fiber well. The prior work by the authors compared other fibers and the performance of PVA at high strain rates was close to that of the aramid. The purpose of the study was to confirm use of the four parameter Weibull function in characterizing the PVA fiber. The results show the comparison to be valid. This may be true for these conditions but outside of these conditions more data would need to be validated to use in design of a protective system. The failure mode of PVA is similar to that of aramid showing the ability to accommodate high strain rate and possibly be a good candidate in protective systems.

5.2 Failure mode related to processing

Another failure mode can be seen after the fiber is processed. The ability of the fiber to maintain its strength and impact properties after weaving and finishing is crucial in the design of the system. Sanborn and Weerasooriya conducted a study to quantify how Kevlar® KM2 600 denier yarn responds to the process of weaving, twisting and finishing [22].

Additional studies on twisted yarn resulted in a “twist multiplier” (TM) which gives the maximum strength and is used for correlation studies to untwisted yarn. This study compares yarn taken from a plain weave fabric and compares the strength to unwoven yarn. Warp and weft samples were taken from a fabric sample after weaving and finishing. Prior to applying the finish the fabric was scoured in hot, soapy water and rinsed. A fluoropolymer was the finish in this case and was used to make the fabric water repellant. Samples were studied using a modified SHPB at quasi-static, intermediate and high strain rates to simulate response of the fiber to impact. In all fiber types the fiber increased in strength as the strain rate increased . The authors postulated the difference could be due to the fiber diameter. In their study the authors measured several fibers in multiple locations along the length of the fiber and found the diameter to vary as much as 3.5 μm. This difference could lead to inaccuracies in the reported tensile strength. For low, intermediate and high strain rates the unwoven yarn was stronger. The weft yarn saw a reduction in strength of approximately 3 - 8% while the warp yarn exhibited a 20-35% reduction. The reduction is attributed to the various manufacturing processes to produce a fabric. Other factors included the crimp in the weave pattern and the friction of the yarn sliding over one another. The variability in the fiber could also contain defects which could contribute to the reduced strength. To determine the effect of processing, multiple yarn gage lengths (2, 5 and 10 mm) were used. For all fiber types the tensile strength decreased with gage length. The authors concluded that at gage lengths greater than 10 mm the defects are evenly distributed and did not show a length scale dependence.

Modulus values were obtained as a function of strain rate. The unwoven and weft yarn exhibited an increase in stiffness as the strain rate increased. Since yarn may become twisted

in processing yarn was also tested in a twisted state. The twisted yarn was tested at the same strain rates as the untwisted with no increase seen in tensile strength across the different strain rates. Although prior studies did show an increase in tensile strength, the authors explained it may have been due to frictional interaction of single fibers away from the break point. The conclusion of the study was that for all strain rates the tensile strength and stiffness of the yarn were affected by processing. The warp direction suffered the most having lower modulus and strength. This is expected as it is under constant tension and the weft yarns are inserted while the warp yarns are lifted and lowered during weaving.

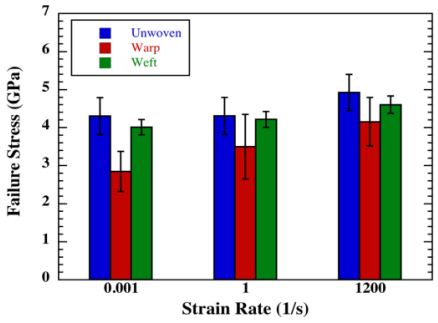

Figure 18 Effect of strain rate on tensile strength in unwoven yarn, warp and weft after weaving. (Reproduced from: Sanborn et al., ref 23)

It is known in the manufacturing sector that processes affect the overall properties of the fiber and specifically that the warp will experience more damage as it is continuously being abraded in the loom during weaving. This study did quantify that the distribution of defects along the fiber axis become normalized above 10 mm.

6 GAP ANALYSIS OF CURRENT FIBER TYPES IN USE AND PROPOSED RESEARCH

Numerous studies have been performed to understand the properties of p-aramids and applications to incorporate their properties into protective systems. Other high strength, high modulus fibers have been studied including UHMWPE, UHMWPP, poly(p-phenylene-2,6-benzobisoxazole) (PBO), and others. Recent studies [14,15,16] evaluated hybrid yarns, surface treatments, commingling, and incorporation of nanomaterials as a means to improve strength properties. Improvement of strength properties was observed in some cases but typically only incremental change was obtained. However, the studies were isolated in their approach. No study combined a surface modification or incorporation of nanomaterials and another fiber with the p-aramid. Furthermore, experimentation and testing was often limited to low velocity testing.

As there are no accepted intermediate test methods I conducted an initial study to evaluate the activation energy of the fiber as encapsulated in a matrix. Individual yarn samples were encapsulated in epoxy. Specimens taken from the master sample were cut to length for the DMA 3-point bending fixture.

The activation energy of the yarn could show how much energy would be required to break the sample using 3-point bending thermal dynamic mechanical analysis. Each fiber type was tested at various frequencies on a Perkin Elmer DMA 7e. A shift in T_g was observed but was inconsistent. The actual mechanism of the T_g shift was most likely the interfacial bond of the fiber to the matrix and thus would not be useful to evaluate the tenacity of different fiber types. This gap may be filled by testing sonic modulus of the fiber as this is a direct measurement of the modulus of the yarn.

Different yarns singly may not have the desired mechanical properties. But combining different yarns by commingling may provide combined properties that meet or exceed the performance of the separate fibers. Additionally, nanoparticle incorporation in the fiber to increase the frictional interaction between fibers in a yarn was shown to improve impact performance. This raises the following questions:

Would an improvement be realized by a true hybrid material?

Would impact properties and projectile penetration be improved from commingling of PVA and KM2+coupled with the interaction of graphene oxide incorporation?

What is the role of the materials in the hybrid system on improving impact toughness?

Research of Kevlar commingled with PVA having GO incorporated as a frictional component could evaluate the potential to increase the energy dissipation of a protective system. However, additional research on intermediate test methods is needed to understand the fiber interactions and resulting fabric strength prior to ballistic testing.

7 RESEARCH MATERIALS AND PREPARATION

The yarn used in this study is KM2 Plus® 850 denier manufactured by DuPont. The PVA is a high strength, high modulus yarn manufactured by Kuraray. Graphene oxide 2mg/ml solution was prepared at North Carolina State University under supervision by Dr. Wei Gao. A modified Hummers method [23] was used to prepare the GO solution followed by filtration through dialysis media for purification.

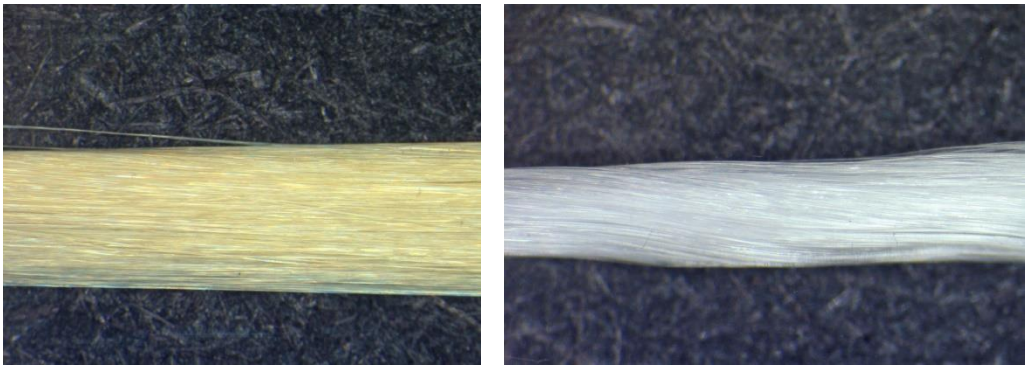

Figure 19 a)KM2 Plus® yarn as received; b) PVA yarn as received

7.1 Yarn preparation

Commingling of the KM2 Plus® and PVA was performed using air jet equipment where the different input raw materials are fed through a drawing zone. The separate yarns are drawn into the path and overfed allowing a decrease in tension, passed through air jets where the two yarns are simultaneously opened allowing filament from both yarns to intertwine, fed to a delivery roll for final combination then fed to the wind up unit.

Twisted yarn used in the study for all yarn types was twisted on a ACBF ring twist frame with a 2.6 S twist per inch.

Figure 20 Sections of commingled yarn showing yarn bundle changes, incorporation of PVA yarn in KM2 Plus® bundle.

.

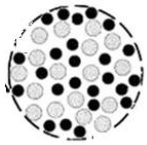

Figure 21 Schematic of typical commingled yarn showing relative dispersion of both fiber types.

7.2 Graphene Oxide Treatment

Individual yarn was fed from the package through an eyelet into the graphene oxide solution then into an oven at 162^0 C to allow the yarn to dry. (Figure 24) Exposure of the yarn to the heat was less than 3 seconds so as to not degrade the PVA or KM2 Plus® based on manufacturers listed melt temperatures. Packages were allowed to air dry for final testing.

Figure 23 – 25 show dispersion of the graphene oxide in the yarn bundle by microscope and SEM.

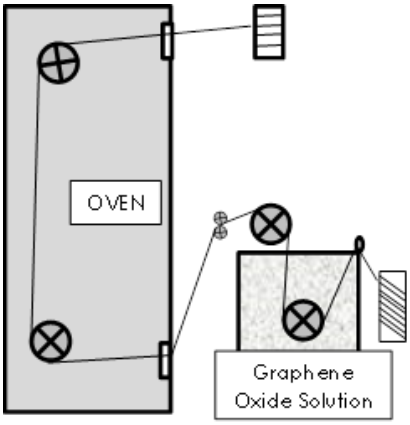

Figure 22 Schematic of process flow for graphene oxide treatment of yarn.

.

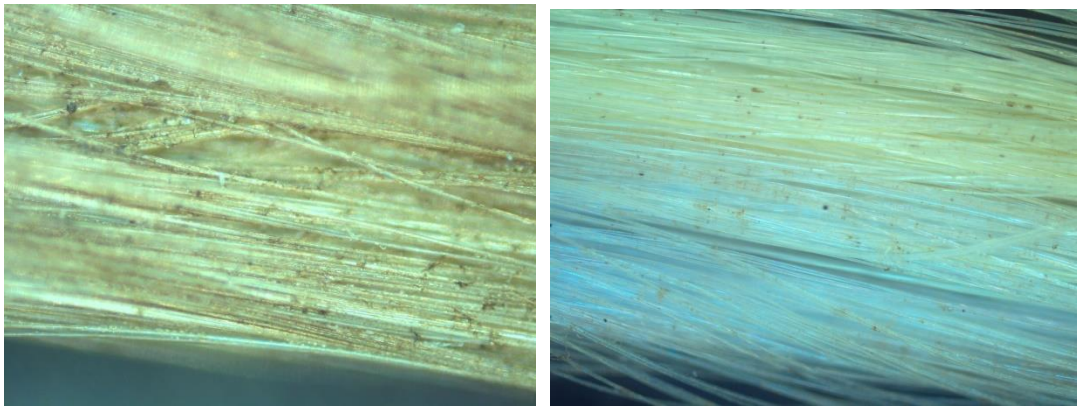

Figure 23 GO dispersion in fiber bundle a) 2mg/ml solution treatment b) 1:10 GO dilution

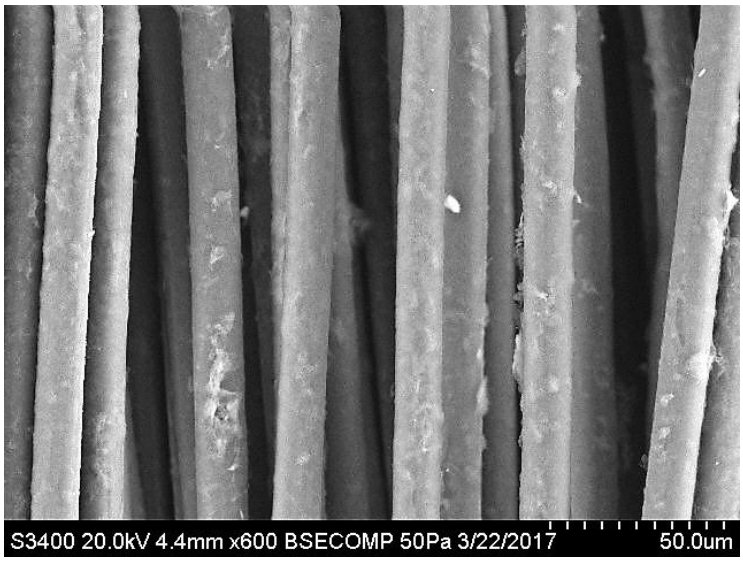

Figure 24 SEM image of commingled KM2 Plus® & PVA with 2mg/ml GO solution treatment.

Figure 25 SEM image of KM2 Plus® & PVA with 1:10 dilution of 2mg/ml solution

8 QUASI-STATIC TESTING OF MECHANICAL PROPERTIES

8.1 Introduction

Yarn mechanical properties (including tensile strength, modulus, yield point and elongation) are key in determining final product design and application. Tensile testing of yarns yields the force required to break a yarn. High performance yarns used in high strain rate applications require a combination of properties as the amount of energy required for failure is as critical to the application as is the mode of failure. Ballistic type events require both impact toughness, plastic deformation absorbing energy prior to fracture, and tenacity, or specific strength, (i.e. ultimate force to break fiber per linear density) due to the high strain rate. The strain rate effect, or measure of rate of physical change within the fiber bundle, is a meaningful way to evaluate high performance yarns.

The ability of viscoelastic yarns to absorb energy, elongate and transfer the load due to the high strength to weight ratio make them suitable for ballistic systems. For viscoelastic yarns the elastic response is associated with load bearing and the viscous response is associated with energy damping. While undergoing deformation the viscous response of the material resists shear flow and will increase strain with time as stress is applied. The elastic response will strain instantaneously and return to the original state after the stress is removed. The polymer chains under stress untangle, rearrange, slide and straighten leading to permanent deformation. [2] As the chains move the fiber necks permitting more sliding at a lower stress.

8.2 Viscoelastic materials and their behavior

Kevlar® and high strength PVA are viscoelastic and exhibit time dependent strain. [24] The high tenacity of KM2 Plus® and PVA arise from the high degree of orientation of the polymer chain. In the p-aramid fiber the structure (Fig 15) alternates between aromatic ring linkages and linear group linkages. Those segments with -CO-NH- are lower in covalent bonds than the segments with aromatic rings. Additionally, hydrogen bonding between molecules in linear segments have strong interactions, leading to greater stiffness of the fiber. [4] This type of bonding sequence leads to anisotropy of the fiber along its axis. The mechanical properties of KM2 Plus® along the axis perpendicular to normal are considered isotropic in this direction. Several models describing viscoelastic behavior including Maxwell model, Kelvin-Voigt model and the Standard Linear Model [25] are utilized in design allowing prediction of material response under different loading conditions. An empirical viscoelastic model can be constructed for materials through a series of experiments to relate stress, strain and time. [26]

Using Hooke's law for linear elastic behavior

$$\sigma = E\varepsilon \tag{3}$$

where:

σ = stress,
E = modulus
ε = strain

and for viscous materials

$$\sigma = \eta \, d\varepsilon/dt \quad (4)$$

where:

η = viscosity as these materials exhibit creep.

The coefficient of viscosity, η is the slope of the stress strain rate curve for a Newtonian fluid. Kevlar® and PVA are viscoelastic and the relationship between stress and strain can be written as:

$$\sigma = \sigma(\varepsilon, \dot{\varepsilon}) \quad (5)$$

showing the relationship of stress to strain and strain rate. As stress is held constant strain will increase with time and conversely show relaxation as strain is held constant the stress decreases with time. In cyclic loading viscoelastic materials also exhibit hysteresis.

Much work has been performed to determine the nature of the viscoelastic behavior of Kevlar® as well as high strength, high modulus PVA. It has been shown that Kevlar® will respond in a linear viscoelastic manner under stress higher than 40% of the average breaking load. Below 40% of the average breaking load the behavior is nonlinear creep. [25]

8.3 Static Tensile Testing (Low strain rate)

Fundamental quality checks of high strength yarns include quasi-static tensile testing based on ASTM standards. Standards for yarn testing indicate the equipment type and required test parameters. Performance of polymeric yarns may exhibit temperature dependence therefore

the equipment may be modified to accept a temperature chamber for testing at different temperatures. There is provision for various loading rates in these standards but testing using constant rate of extension (CRE), constant rate of traverse (CRT) or constant rate of loading (CRL) are at strain rates significantly lower than typical ballistic events. While tensile testing does not imitate the time scale of a ballistic impact event useful information on the viscoelastic response can be obtained.

8.4 Tensile Strength versus Toughness Trade-off

The quest for stronger and tougher materials in ballistic applications continues. Materials that are strong resist stress to non-recoverable deformation (plastic deformation). Material toughness is indicative of the ability to withstand limited deformation (ductility) as the stress is dissipated locally. Materials with high strength tend to be more brittle while lower strength materials have more ductility and deform more readily. The combination of strength and toughness is a trade-off between these two properties as the molecular bonding giving rise to these properties can be mutually exclusive.

Intrinsic properties of Kevlar KM2 Plus® and high strength high modulus PVA include a high degree of polymer chain orientation. Hydrogen bonding between parallel polymer chains makes the process of deformation more difficult. The result is mitigation of locally high stresses through effective dissipation of the stress. Material toughness can be calculated by measuring the area under the stress strain curve from tensile testing and will have units of energy per volume of material. [27] For composites the toughness can be measured by dynamic mechanical testing of a laminated or consolidated specimen using a double

cantilever beam or 4-point bending. The Mode I (G_{Ic}) and Mode II (G_{IIc}) interlaminar fracture toughness is calculated as critical energy release rate. [28]

Energy loss is key to high velocity impact events therefore the mechanism of energy dissipation is not isolated to the ultimate tensile strength of the yarn. The area under the curve represents the work done by the yarn in energy absorption up to failure. The greater the area the more energy dissipated. Hybridizing two yarns to create a combination of high strength from both yarns along with increased elongation capacity could result in an improved yarn. The load would be transferred first to the stronger yarn until failure, followed by load transfer to the second fiber. In this study the PVA is high strength, high modulus possessing a greater elongation characteristics than the KM2 Plus®. As the load is transferred to the second fiber, the PVA elongates until rupture thus increasing the effective toughness. The contribution of GO is that of a frictional component as the presence of GO in the yarn bundle and between yarns in a woven fabric during movement of the fibers increases the contact force perpendicular to the interface increasing energy absorption.

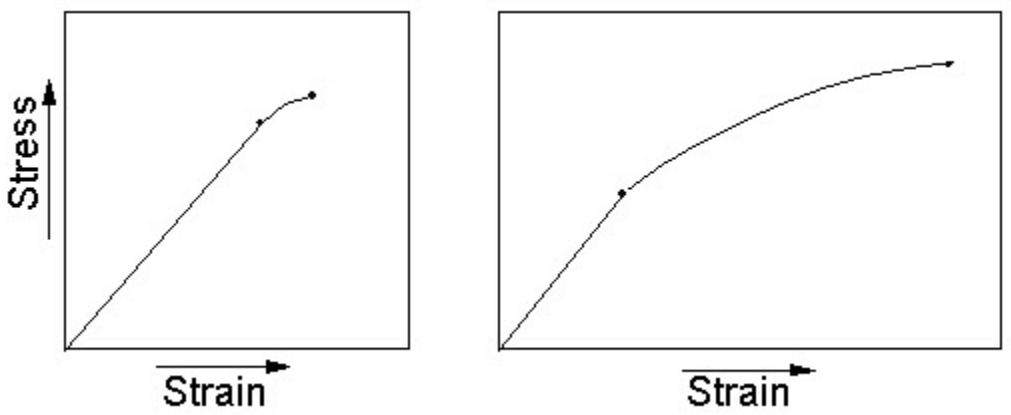

Figure 26 Stress strain curve for a) brittle material and b) ductile material

8.5 Experimental Methodology

Static (low strain rate) tensile testing was performed on an Instron 3365 equipped with a 2 kN load cell. Yarn is mounted in specialized grips known as capstan grips. These grips properly align the specimen and evenly distribute the tension across the curved section of the grip due to the narrow cross section. This prevents test error occurring from premature failure outside the gage length on sharp edges of typical wedge grips. The yarn is pulled at a constant rate of speed per ASTM D579 and D7269 until failure occurs. The strain rate in quasi-static testing is below $1s^{-1}$.The applied load and measured elongation are presented graphically as a stress strain curve. Ten samples for each yarn type , reference KM2 Plus®, PVA, KM2 Plus® & PVA commingled, KM2 Plus® & PVA twisted, commingled yarn with GO and a dilute solution of GO 1:10,were tested to ensure adequate sample data.

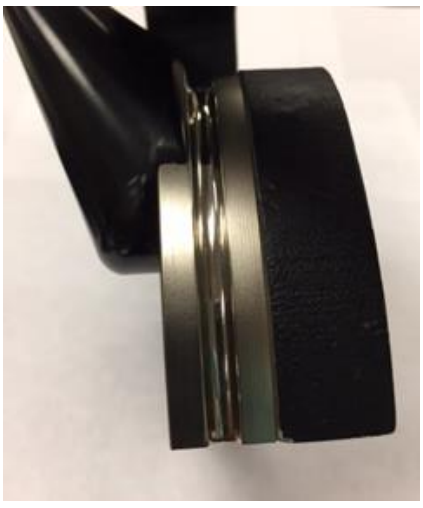

Figure 27 Instron® yarn capstan grips and side view of grip curved surface.

8.6 Results and Discussion

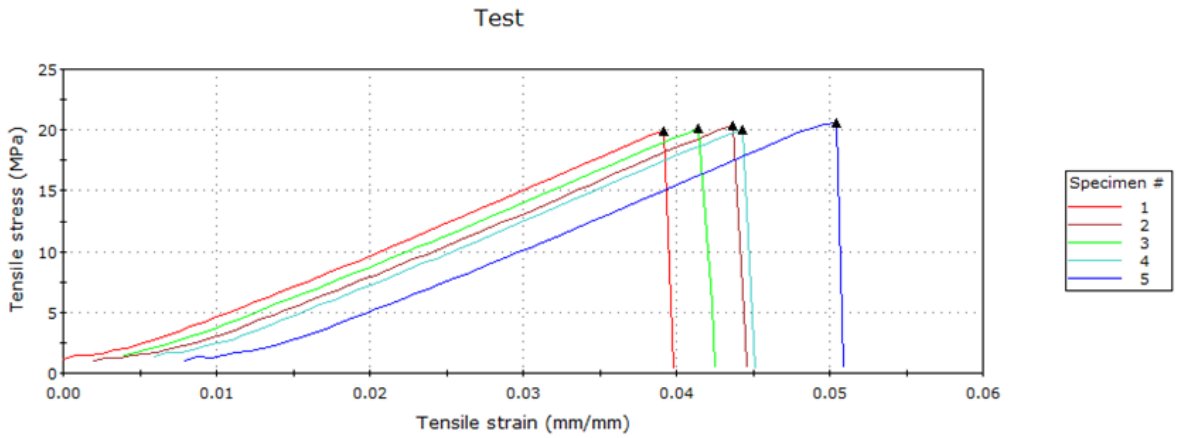

Figure 28 Quasi-static stress strain curve of KM2 Plus® showing five of the ten test samples in the as received state.(Note: Offset of each specimen is added to the data for clarity & does not reflect actual prestrain)

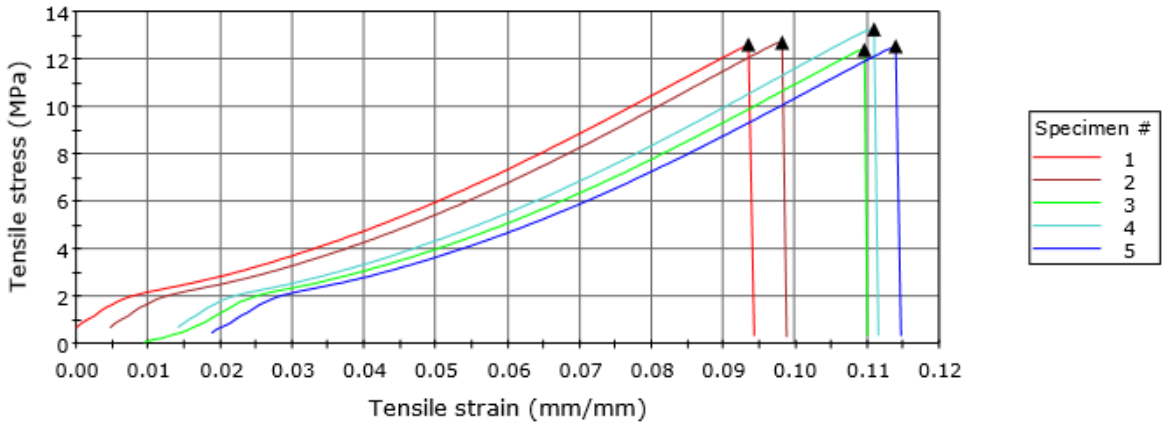

Figure 29 Quasi-static stress strain curve for five of the ten "as received" specimens of PVA yarn. Note greater elongation of PVA than aramid yarn. .(Note: Offset of each specimen is added to the data for clarity & does not reflect actual prestrain)

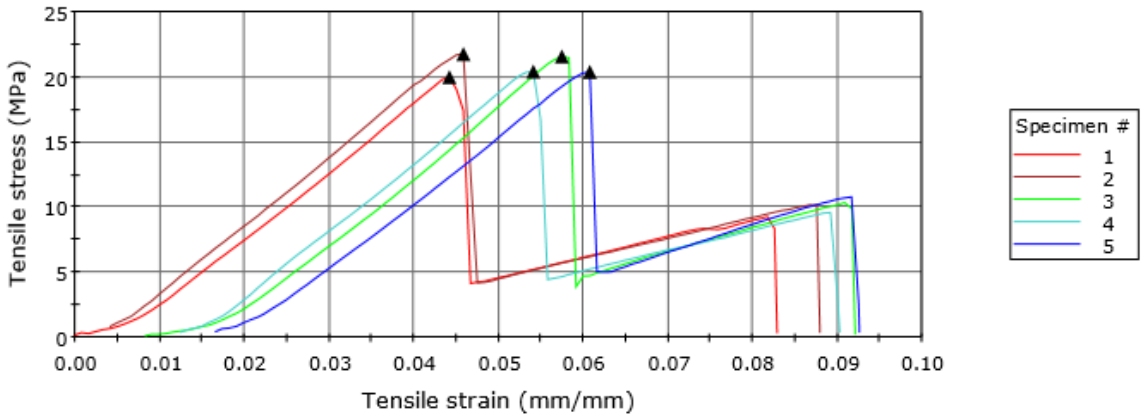

Figure 30 Quasi-static stress strain curve for five typical hybrid (commingled) yarn showing initial break of aramid followed by elongation and break of PVA. .(Note: Offset of each specimen is added to the data for clarity & does not reflect actual prestrain)

Figures 28 – 30 show five of the ten or more samples tested showing typical stress strain curve for the yarn types shown. Static tensile test data confirmed KM2 Plus® had lower

elongation prior to rupture in the “as received” and twisted state than PVA. The PVA did exhibit greater strain but no significant difference was found between the “as received” state and twisted state. There was greater tensile strain in the commingled state which indicated a change in the fiber bundle. This was confirmed in the tenacity data as the twisted yarn form for KM2 Plus® and hybrid twisted yarn had higher tenacity values. One deviation was the tenacity of the twisted PVA yarn which did not change significantly from the “as received” state.(Fig 31) In each yarn type the commingled form had lower tenacity values. The hybrid (commingled) yarn with graphene oxide treatment and a dilution of 1:10 of the graphene oxide treatment had a slight decrease in mechanical strength as compared to the hybrid yarn with no treatment.

Twisting of the fiber added integrity to the yarn bundle as a whole. [54,55] However, there is an optimum level of twist beyond which mechanical properties will decrease per ASTM D7629. [29] The increase in mechanical properties arises from the individual filaments in twisted yarn constrained more closely through radial forces and interyarn friction. [30] The compression in the transverse direction could change the failure mode by facilitating an individual filament failing in several axial locations. [31]

The contribution of GO as a frictional component to increase interyarn friction was not evident in quasi-static tensile test. No significant change in specific strength of commingled with and without GO treatment indicates the GO was not participating as a frictional component. The slight reduction in tenacity shows the treatment did not create a stiffer response from increased friction in filament movement.

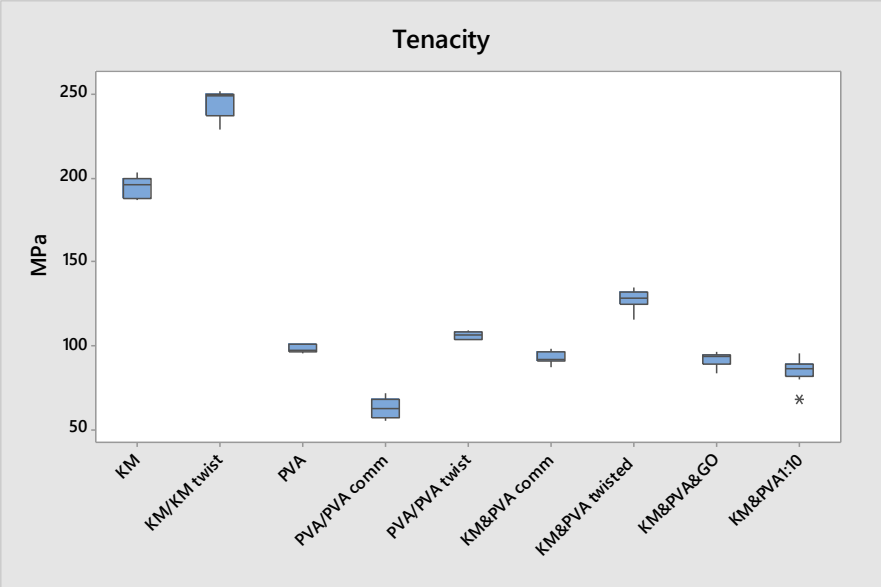

Figure 31 Tenacity (specific strength) comparison for each yarn type.

Tenacity data for twisted yarn consistently showed significantly higher values over commingled yarns. Even though the denier of the twisted yarn versus commingled was the same, the yarn bundle geometry was quite different. Commingled yarn have been opened and may no longer be cohesive disrupting the ability of the filaments to act as a single unit regarding mechanical properties. The specific strength of twisted versus commingled yarns showed twisted yarns to have a greater increase in strength. Hybrid yarn with the graphene oxide again exhibited a decrease in tenacity and toughness properties with the dilute solution treatment showing more of a decrease. (Fig 31 & 32)

Strain energy per unit volume for the hybrid yarn had two peaks (Fig 31) with the first peak showing the break of the KM2 Plus® followed by the elongation of the PVA until rupture. Toughness follows the same trend as tenacity with the twisted yarn having higher toughness than the commingled yarn. This trend follows prior experimental work to determine the

effect of twist on yarn mechanical properties. [54,55] Yarn twist has been determined to contribute to an increase in yarn strength by adding integrity to the bundle. The increase in mechanical properties results from the anisotropy of the yarn. This anisotropy yields a modulus that is greater in the longitudinal direction than the transverse direction. Anisotropic yarns, when twisted, will exhibit sizeable contraction in the lateral direction under axial extension. [35] Under extension the change in the helix angle results in yarn torque. As the yarn is constrained by the twist radial compression occurs. The compressive force increases the capacity to carry the load as the force is transferred through the outer filaments to the inner filaments. [31]

Models proposed by Platt, [32] Hearle [33] and others to correlate yarn twist to yarn modulus

incorporate the relationships of twist yarn geometry, yarn or filament extension, axial tensile force, lateral contraction and transverse forces. Recent models proposed by Rao et al [34] also incorporate the anisotropy of the yarn and have reported better agreement with actual experimental values. Their findings indicate the "anisotropic ratio" as the critical component identifying dependency of twist on yarn modulus. The anisotropy ratio is defined as the "ratio between the axial modulus and radial shear modulus". [34]

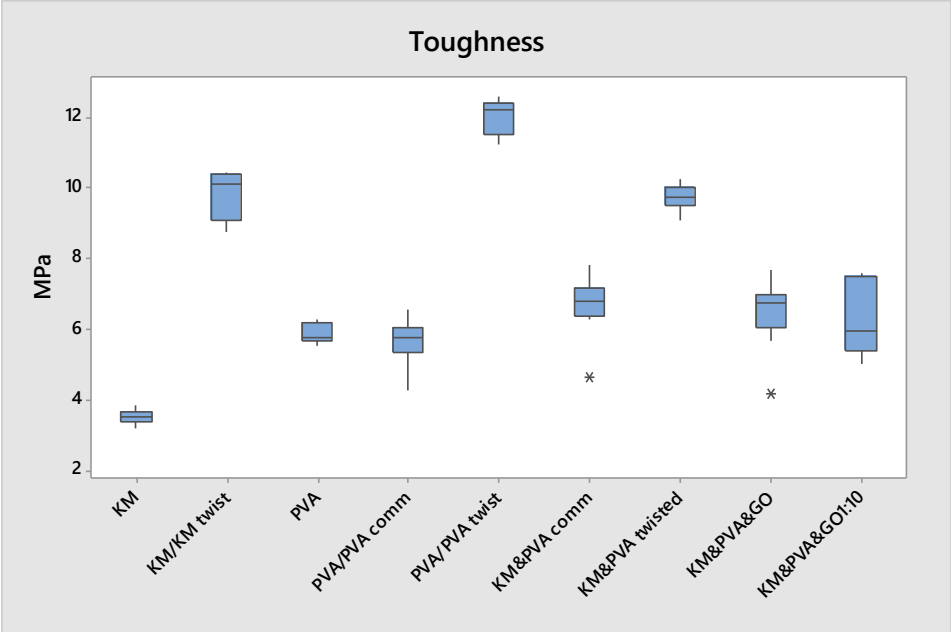

Figure 32 Toughness (area under stress strain curve) for all yarn types.

8.7 Conclusion

Twisted yarn consistently had greater mechanical properties than commingled or GO treated yarn as tested by quasi-static tensile test. This may have been caused by disruption of the commingled yarn as was seen by comparing the tenacity of the individual PVA yarn with the values of the "as received" and twisted yarn. The presence of graphene oxide did not show a contribution to interyarn friction or dissipation of energy in these tensile tests based on the toughness values for each type.

9 DYNAMIC MODULUS TEST METHOD USING SONIC VELOCITY

9.1 Introduction

There are several methods to determine Young's modulus of a material. These include static tensile, dynamic (resonant frequency), ultrasonic echo pulse method and nanoindentation each having advantages and disadvantages. Dynamic or sonic modulus is the use of the fundamental vibrational frequency of a material to determine physical characteristics such as modulus, molecular orientation and material anisotropy. It is based on time-varying deformation or vibrational motion of atoms as they are stressed from their equilibrium positions. [36] Systems that measure sound speed in materials are comprised of a pulse transmitter, pulse receiver, meter, timing circuit, transducers (mounted piezoelectric crystals) for placing sample in sonic path and converting to electrical signal. (Figure 33)

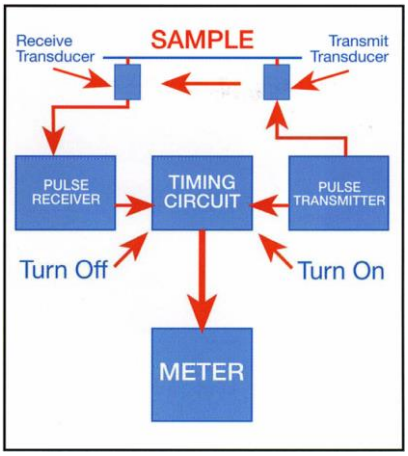

Figure 33 Sonic velocity pathway courtesy Lawson Hemphill.

Measurement of dynamic modulus by sonic velocity testing has an advantage of being independent of cross sectional area as $E = \rho c^2$. [37] It is a direct measure of the modulus rather than indirect, as is the static or tensile test, which gives load versus extension.

The molecular composition of a material determines its physical properties and therefore determines the velocity at which sound propagates through the material.

9.2 Basic Principles of Sonic Velocity Test Methodology

For a given pulse the wave propagation can be seen as an extension of Hooke's law of elasticity that for deformation the displacement resulting from the deformation is directly proportional to the load. The yarn is considered as having a cross sectional area and a stiffness. [35]

Basic sonic modulus principles

Calculating the velocity of sound per ASTM requires measuring length and time as:

$$C = \Delta l/\Delta t \quad (6)$$

$$C = \text{Distance (cm)} \times 10^{-5}/\text{transit time } (\mu s) \times 10^{-6} \quad (7)$$

$$E = \rho C^2 \quad (8)$$

$$(E/\rho) = C^2K \quad (9)$$

Where:

C = sound velocity in km/sec
K = constant conversion factor (11.3)
E = Young's modulus of elasticity; ρ= density (g/cm3)
E – grams/denier = $(E/\rho) = C^2K = C^2$ 11.3

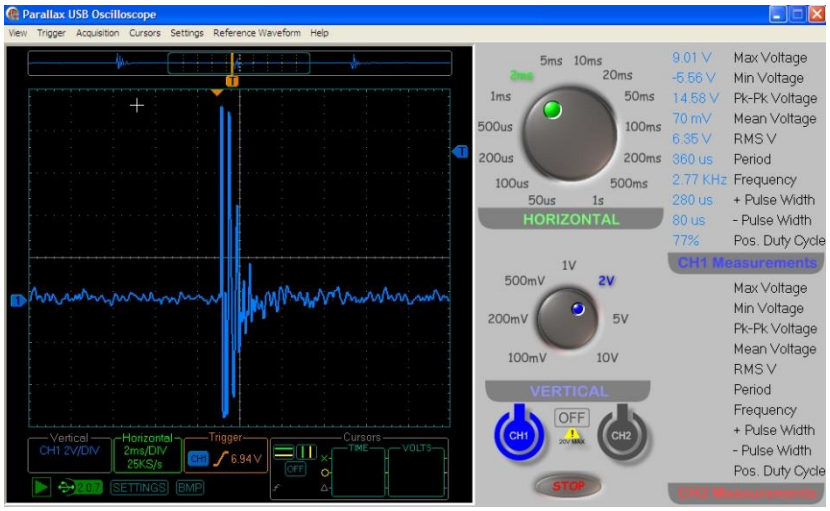

Figure 34 USB Oscilloscope image of waveform in KM2 Plus. Image shows voltage as a function of pulse time through material.

Ryan and Postle [38] researched and identified the theory supporting sonic velocity measurement of dynamic modulus. Materials with strain rate sensitivity show an increase in

modulus as the sonic pulse rate converges on the velocity of the stress wave propagation of that material. The predominant vibrational modes are longitudinal, torsional and flexural for a composite system. [36] Longitudinal wave theory indicates that the waves are predicted to spread in an elastic rod structure as per equation 8.

Ballou and Silverman [39] state those systems with both plastic and elastic behavior will not produce unbiased test values, because, when tested with static procedures the low loading rate in those tests allow the fiber to stretch thereby augmenting polymer chain orientation. Therefore, study of elastic properties is not well adapted to quasi-static testing but necessitates a high strain rate to reduce relaxation of the polymer chain.

In a ballistic event the system is impacted by the projectile typically transverse to the fiber axis. The energy from the projectile is transmitted to the system in waves initiating at the point of contact. The longitudinal strain wave propagates outward from the contact point at the speed of sound of that material parallel to the direction of propagation. The transverse or shear wave is slower than the longitudinal wave and travels perpendicular to the direction of propagation.

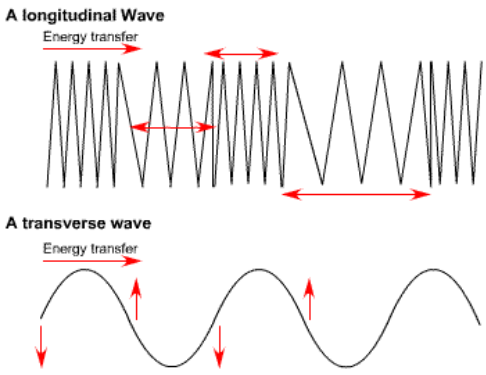

Figure 35 Longitudinal wave propagation and transverse wave propagation. (Reproduced from www.socratic.org)

9.3 Experimental Methodology

Testing was performed on a Lawson Hemphill Dynamic modulus Tester LH 551, see Figure 39. The yarn is fixed on one end, passes through the wires of the transmit and receive transducers to a small wheel and is fixed to a weight (100g) providing enough force to keep the yarn in tension and allow transmission of sound but small enough so as to not stop or reduce the sonic pulse. The sample was tested at distances from 10 to 20 cm. The transducers consist of quartz (piezoelectric) crystals which send and receive the sonic pulse. As electric current is applied to the crystal this causes the crystal to rapidly vibrate. These vibrations produce sonic waves traveling outward. Crystals upon being hit by sound or pressure waves emit electrical current which allow measurement of the time between pulse send and receipt. The length between the transducers is variable allowing measurement of the transit time of the pulse between the transducers giving material sonic velocity. Transit time of the pulse through the sample between transducers is recorded as per ASTM E1875. The data is plotted as distance versus transit time with the slope of the linear regression line as the sonic velocity in km/sec. Modulus calculated as per equation 8.

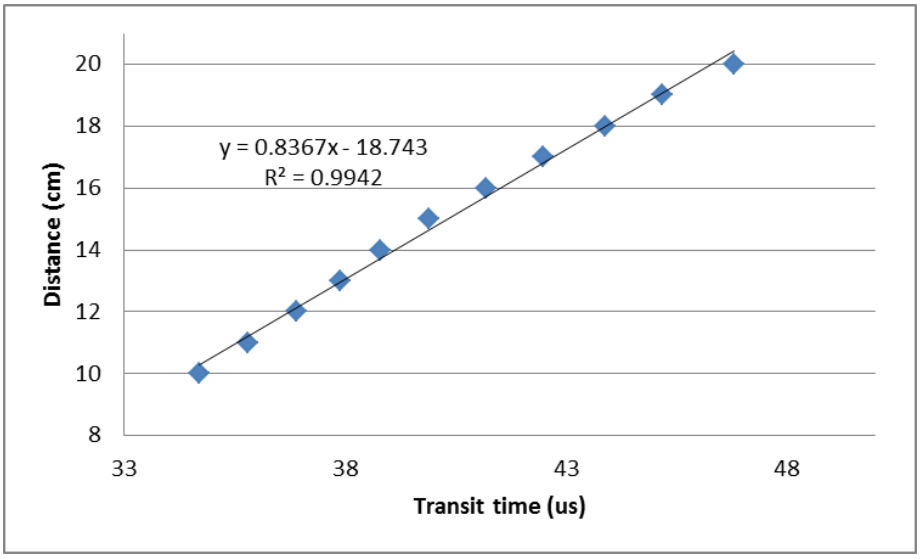

Figure 36 Plot of sonic pulse transit time as a function of distance with linear regression curve fit.

9.4 Results and Discussion

Sonic velocity of untreated commingled yarn was 5.655 km/sec and twisted yarn had a sonic velocity of 6.785 km/sec which was lower than the 8.425 km/sec of the "as received" yarn. GO treatment of the reference KM2 Plus® yarn had an 11% reduction in pulse propagation, and thus the modulus, and a further reduction was seen in the commingled reference yarn with GO treatment. Twisting and commingling of the yarn changes the yarn bundle configuration acting as a change in path length reducing the effective velocity in the yarn. The addition of GO, as seen by a reduced velocity, also acts as a hurdle to the sonic pulse. Of interest is the trend of KM2 Plus®. Sonic velocity is diminished as follows: KM2 Plus® as received > KM2 Plus® + GO > KM2 Plus® twist > KM2 Plus® + GO commingled > KM2 Plus® commingled. Within this trend the standard deviation of the commingled yarn is greater than the twisted yarn. However, the commingled form had lower sonic wave

propagation indicative that yarn bundle configuration is a factor in propagation of the sonic pulse and therefore the energy. All of the hybrid combinations had similar sonic velocity values with GO treated hybrid yarn having the lowest velocity. Hybridization provides multiple path lengths by scattering the pulse. GO in this test does indicate the ability to impede the sonic pulse.

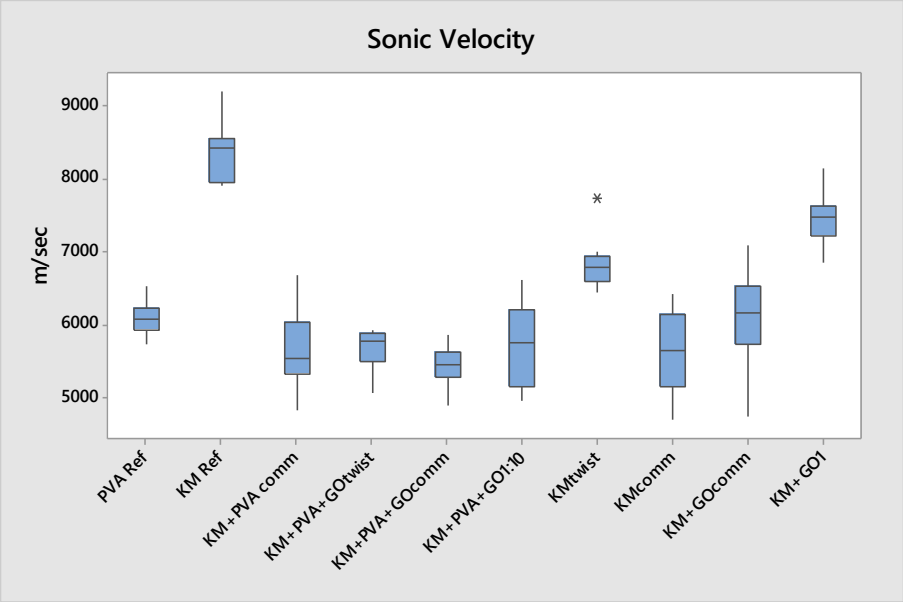

Figure 37 Sonic velocity in m/sec of yarn types as tested on Lawson Hemphill LH551.

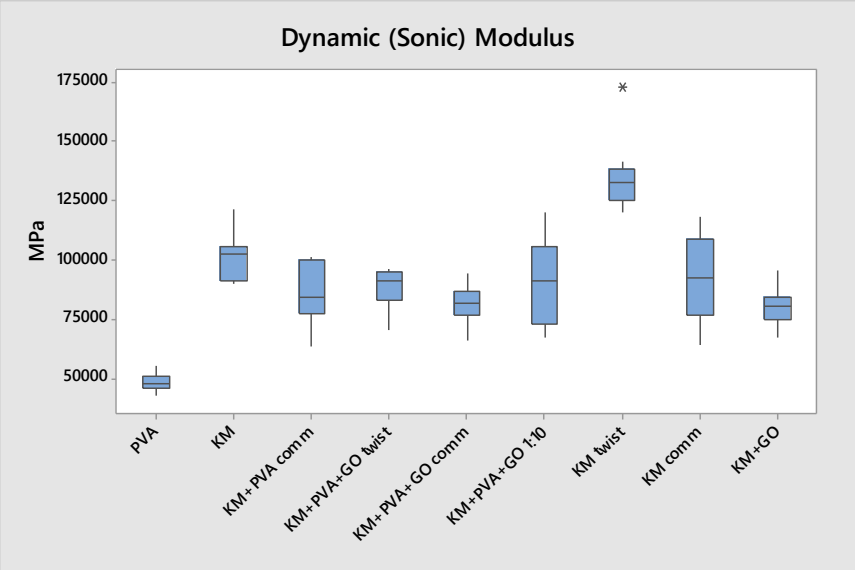

Figure 38 Dynamic modulus calculated from sonic velocity for each yarn type.

Young's modulus as calculated from the sonic data utilizes the yarn density. The normalization of the data as a function of linear yarn density shows the modulus at the speed of sound in the material for twisted KM2 Plus® as the highest. This follows the trend seen in static tensile testing. However, treatment of Kevlar® with GO reduces the modulus from that of the as received state. During treatment of the yarn with GO the yarn bundle may experience changes such that the yarn bundle no longer acts as a cohesive unit lowering the modulus. The hybridized yarn types were all within the same standard deviation of the yarn treated in the dilute GO solution with the twisted yarn having the highest mean value.

9.5 Conclusion

Twisted yarn again exhibits higher resilience over the commingled yarns. Treatment with GO has an effect on standard yarn lowering the modulus. This reduction indicates changes to the yarn bundle can shift the sonic velocity but does not provide means to change the ability of

the material to deform and absorb energy. Dynamic modulus values of the combined yarns seem to follow the rule of mixtures as yarn types having commingled yarns are within the average sum of the moduli of individual input yarn.

Sonic velocity measurement indicates that GO does have an effect in reducing the velocity of the pulse through the material. However, the GO treatment is not shown to contribute to an increase in modulus at high strain rate. The noted reduction of KM2 Plus® with GO treatment shows that although the GO does shift the propagation of the pulse in the material it does not translate to a higher modulus.

10 YARN PULL OUT AND THE ROLE OF FRICTION

10.1 Amonton's Law as applied to yarn friction

Frictional forces between surfaces cause energy loss as described by Amontons' law

$$F = \mu N \tag{10}$$

where :

F = frictional force
μ = frictional component
N = normal force

Amontons' first law states the frictional force is independent of contact area between two bodies sliding on one another and the second law states frictional force is proportional to the load applied perpendicular to the surfaces. The source of friction could be from molecular attraction or adhesion from molecules on each surface or the particulate mechanically displacing material from the surface of the fiber when under pressure. [40] Static friction (force needed to start sliding) as compared to kinetic or dynamic friction (body in motion) can differ especially at high strain rates.

Interyarn and intrayarn friction both contribute to impact energy absorption in a ballistic event. Energy from the projectile is required to overcome static friction putting the yarn in motion. Further energy is expended to move the yarns aside and or cause yarn failure. Following the rule of mixtures the mechanism of energy dissipation in such an event includes the static and kinetic friction (interyarn and intrayarn) as the projectile loses energy to these components.[41]

The tribological effects in woven fabric during impact may be evaluated by yarn pull out testing. Yarn pull out testing has not been standardized and researchers have developed different tools to perform testing. Fixtures vary from wrapping yarn transverse to the individual yarn being tested and attached to weights to a fixture placing a section of woven fabric in tension in the transverse direction. [12,41,42] The purpose is to duplicate the geometric effects of weaving (i.e. crimp and translation) during the impact.

Woven fabrics using high strength yarns have been in use for years with extensive studies performed to characterize their strength properties. [6,10,12,15] An approach to improving the penetration behavior of a protective system has been to utilize modifications to the yarn via shear thickening fluids, [43] carbon nanotubes or other particles [44] intercalated in the yarn system. The purpose is to increase resistance to movement or flow by roughening the surface or through nanoindentation or nanoscratching by the particle on the fiber surface. Addition of particulate is not a significant mass addition potentially allowing improvement of resistance to movement with no substantial weight gain in the protective system.

Modification of the yarn surface friction by particles such as graphene oxide, do not impair the functionality of the yarn and do not add significant mass. Graphene oxide (GO), as used in this study, is an oxidized form of graphene and was produced using the modified Hummers method. [23] The GO has a two-dimensional structure arising from the hexagonal carbon rings fused together appearing as platelets. The oxygen containing groups are prevalent in this single atomic layer material and thereby facilitate dispersion in water. [23] Yarn having GO dispersed on the surface of the fiber may cause an increase in surface gouging at high impact, contributing to the overall mechanism of energy loss by frictional interaction.

10.2 Experimental Methodology

To quantify the coefficient of friction using typical yarn pull out testing does not adequately imitate high impact strain rate. Yarn to yarn friction comparison with and without the GO modification may be tested using dynamic constant tension friction testing because typical fixtures rely on clamp tension to keep a majority of yarns in place possibly having inconsistent tension across the sample. Dynamic yarn friction maintains constant friction on the sample.

Dynamic testing on the Lawson-Hemphill CTT Dynamic Yarn Friction Tester LH 402 provides test data from the full length of yarn tested as the equipment uses dynamic yarn transport keeping the yarn in constant tension during testing. The yarn is pulled from the package to the input rolls and is wrapped around these rolls a specified number of times then fed to a tension arm. Yarn flows from the tension arm and is fed to the yarn twist fixture. Yarn may be twisted a variable number of times based on testing requirements. Yarn twist is centered in the twist guide. As the test is performed constant tension is applied on the input yarn and the change in tension measured as output tension is calculated.

Figure 39 Lawson Hemphill CTT Dynamic Friction Tester LH402 (Courtesy of Lawson Hemphill).

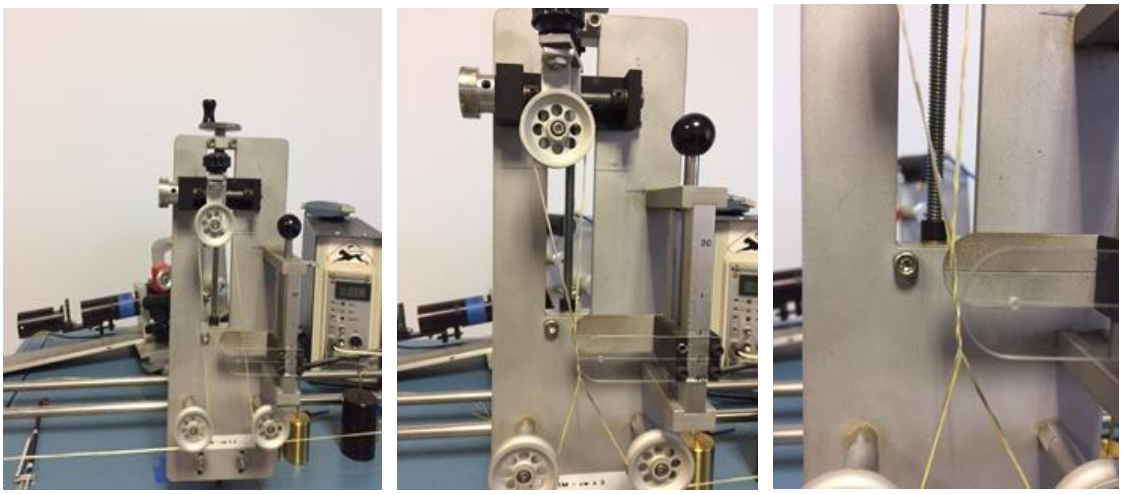

Figure 40 Yarn twist fixture showing a) yarn with no twist, b) yarn with twist and c) insert view of yarn twist.

Coefficient of yarn to yarn friction is calculated as follows per ASTM D3412 test method:

$$\mu = \frac{\ln\left(\frac{T_0}{Ti}\right)}{4\pi(n-0.5)sin\beta/2} \quad (11)$$

Where:

μ = coefficient of yarn to yarn friction
T_0 = output tension
T_i = input tension
β = lower apex angle between two yarns
n = number of wraps

10.3 Results and Discussion

Yarn to yarn friction in fabric occurs at every crossover point between the warp and fill yarns. Determining the degree of shear force as a function of yarn to yarn contact by twisting the strands and creating the effect of crossover points allows evaluation of the frictional effect of surface contact and in this study the effect of GO treatment of the yarn.

Yarn tension profiles seen in Figure 41-44 show the tension output as the yarn was tested. Noted was the very smooth profile of the PVA showing lower increase in friction as the yarn was pulled across itself. The tension profile for the aramid yarn had sections with a brief spikes in tension and the commingled yarn had random sections with irregular changes in tension during the test (perturbations). Commingled yarn treated with 2 mg/ml GO had a smoother tension profile during testing. The same effect is seen to a lesser degree in the dilute GO solution treated yarn.

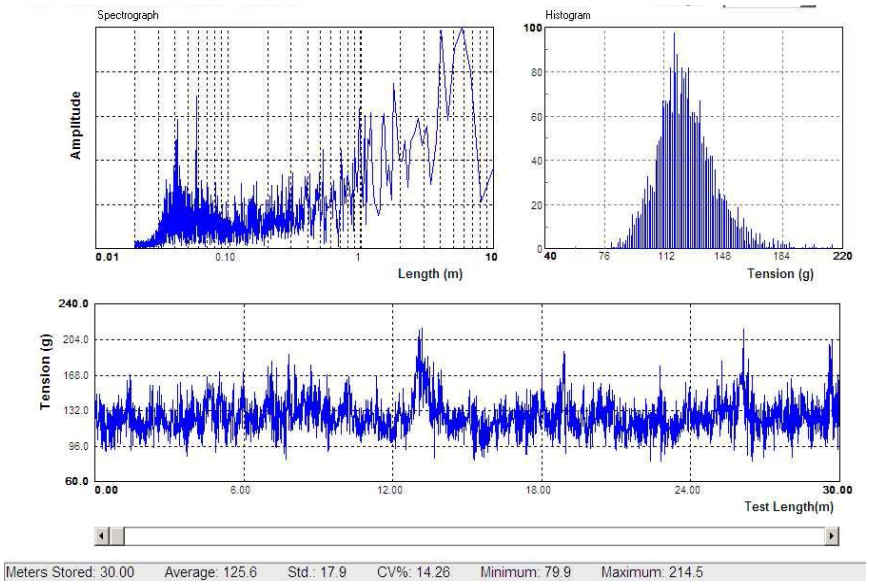

Figure 41 Yarn tension profile for aramid yarn. Note spike in output tension during test.

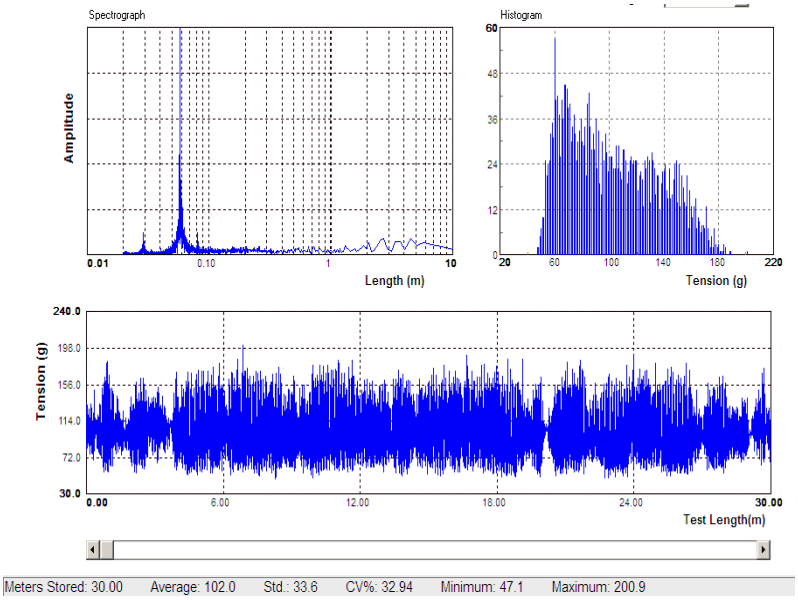

Figure 42 Yarn tension profile for PVA. Note smooth and consistent profile as yarn is tested.

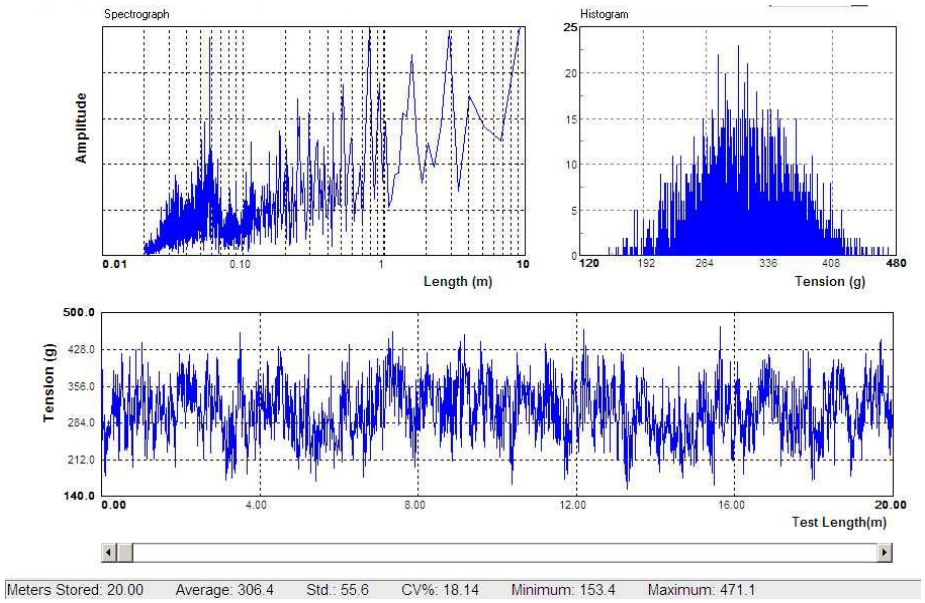

Figure 43 Yarn tension profile for aramid & PVA commingled. Sections with perturbations in tension are seen along length of profile.

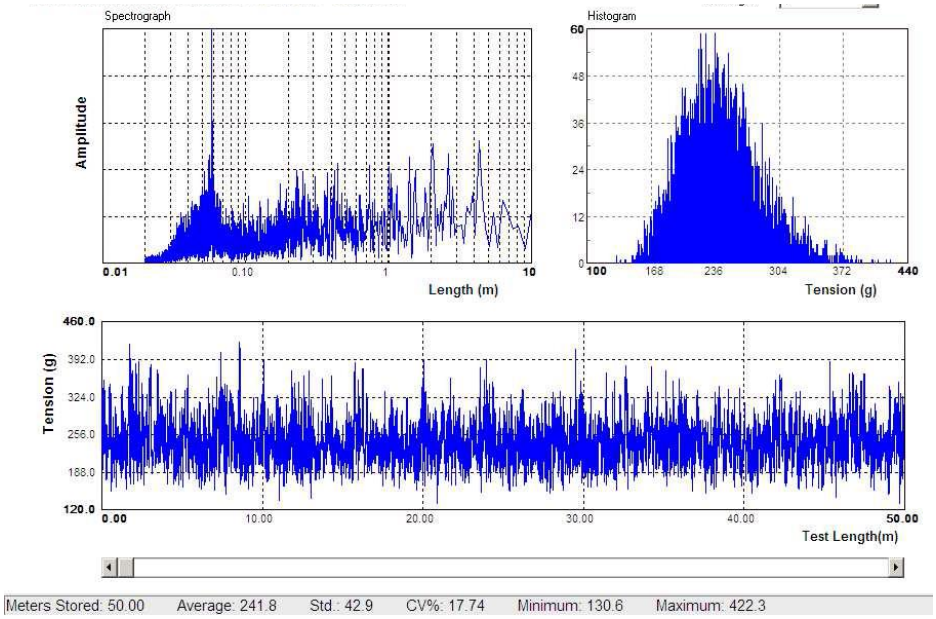

Figure 44 Yarn tension profile for GO treated hybrid yarn. Sections with irregular output tension are smoothed.

.

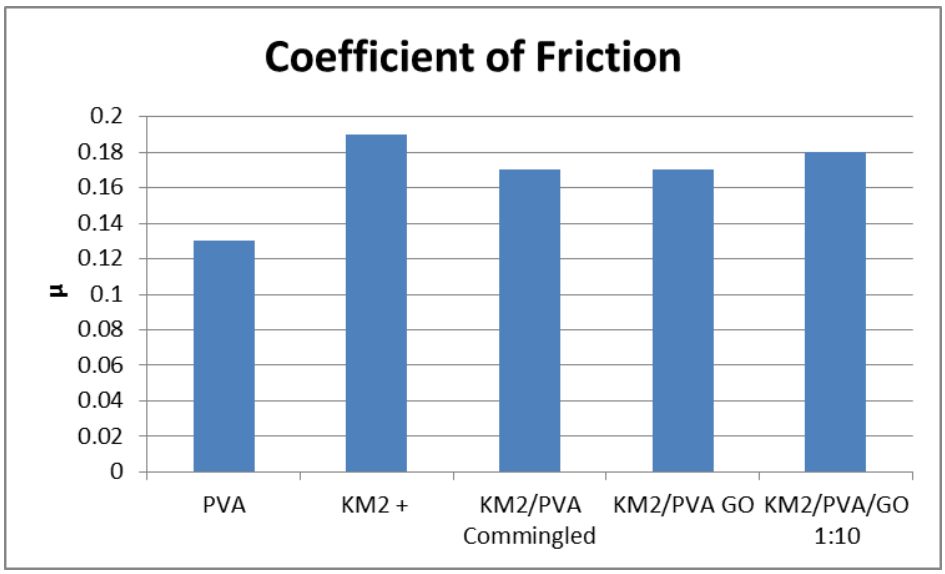

Figure 45 Coefficient of friction comparison of reference yarns PVA & KM2 Plus® with commingled yarn, commingled yarn with GO treatment.

PVA shows the lowest coefficient of friction with KM2 Plus® having the highest yarn to yarn friction. Commingled yarn and GO treated commingled yarns did have slightly lower coefficient of friction but not statistically different than the hybrid yarn treated with the dilute solution of GO. Lack of significant differentiation between all samples, excluding PVA, shows the GO treatment did not have a tribological contribution as would be seen in yarn pull out under high velocity impact conditions.

10.4 Conclusion

Tension profiles of each yarn type show PVA interacting on itself had a smooth profile. This is not the case for KM2 Plus® or the hybrid commingled yarn. The perturbations seen in the profile indicate a frictional component. The commingled yarn treated with 2 mg/ml GO had a smoother profile. The smoothing after initial start-up may indicate the GO is acting more as a lubricant. The average values of the friction at 2x twist do not support GO acting as a frictional component.

11 HIGH STRAIN RATE FABRIC TEST USING SPLIT HOPKINSON PRESSURE BAR

11.1 Introduction

Deformation of materials at high strain rates is usually accompanied by damage and ultimately failure. Yarn mechanical behavior in the regime of dynamic loading conditions may show their viscoelastic behavior in a different manner than at low strain rate testing. Nonlinear behavior can be exhibited in polymers, just as in metals, giving rise to property improvement or failure in the higher strain rate regimes. Deformation is developed from the pressure wave propagating as the load is applied. The same load applied to these materials in quasi-static conditions, leading to localized elastic and/or plastic flow, can be quite different when applied dynamically due to their strain rate dependence. [45]

Initial experimentation by Hopkinson using a long bar was further developed into a tool to measure impact pulse shape. [46] Research by Kolsky changed the configuration to have two long bars and the sample sandwiched between the two bars. [47] The split Hopkinson configuration further studied by Harding expanding on the early work on compression to applications in tension and torsion. Kolsky set forth several assumptions as the basis for analysis of the three waves (incident, reflected and transmitted):[49]

1) Waves propagating in the bars can be described by one dimensional wave propagation theory

$$\frac{\partial^2 u}{\partial \cdot t^2} = V_b^2 \frac{\partial^2 u}{\partial \cdot x^2} \quad (13)$$

2) The stress and strain fields in the sample are uniform in axial direction
3) The sample inertia and the friction effect in compression testing is negligible

11.2 Hopkinson bar basic configuration

The Hopkinson bar equipment set up consists of two long cylindrical bars, incident and transmission, each having the same diameter. A striker bar also of the same diameter is propelled by a gas gun striking the incident bar. This generates a longitudinal pressure wave that travels down the incident bar to the specimen. At the specimen interface part of the wave is reflected back into the incident bar and part is transmitted through the interface due to the impedance mismatch between the bars and the sample. The wave travels to the specimen then into the transmission bar. Strain gages mounted on the incident and transmission bar are used to calculate the force, stress and strain experienced by the sample.

Wave propagation theory is used to determine the stress and strain. Strain rate is obtained from the strain measured in the incident bar caused by the reflected wave. Strain rate variation is achieved through control of input air pressure.

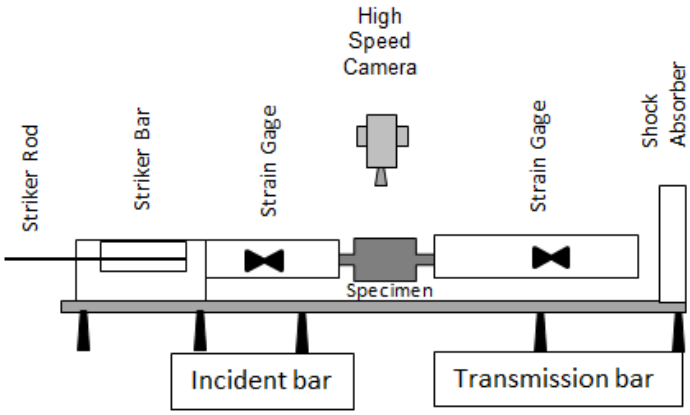

Figure 46 Schematic of Split Hopkinson Pressure Bar showing mechanism of projectile impact and data capture.

Concerns are raised in many studies when performing high strain rate testing of soft materials such as polymers. [50] Very few studies have been performed on fabric and there are no standardized test methodologies or specimen geometry. Ballistic or impact application studies have been done in composites with a variety of matrix materials. [5,6,10,14] Research on the question of specimen configuration have focused on sample size, geometry and means of clamping the sample. [51,52,53] Clamping systems have included epoxy cementing the sample in a customized fixture, glue adhering the sample to plates, glue of a strain gage to the specimen. However, due to the nature of fabric type samples and composites no standardization has occurred. The findings do consistently indicate a small sample size produces repeatable data as the shorter length allows the sample to reach equilibrium more quickly. Small sample size is explained by the Weibull strength effect theory which assumes that material strength for brittle substances is governed by the statistical distribution of defects.[56]

Following the recommendations of these earlier studies [51,52,53] we used a small sample size and insulated the sample from the grip surface and edge to obtain meaningful data.

11.3 Experimental Methodology

Testing was conducted using an REL SHPB. The incident bar is 2.44m long and the transmission bar is 1.88m long. The striker bar is hollow with an inner diameter of 1.91cm and an outer diameter of 2.54 cm. Tests were performed in conjunction with a Photron Fastcam SA-X2 for high speed video. The pulse generator signal for the camera was Stanford Research Systems DG535. An Agilent Technologies DSO 5032A oscilloscope was used for signal recording.

Fabric samples using KM2 Plus® in the warp direction and commingled KM2 Plus® and PVA in the weft direction were prepared in a similar manner as yarn for GO treatment. Small sections (approximately 5" long and 2" wide) were removed from the full width fabric and dipped through the GO solutions. From these larger sections individual sections approximately 3" in length and 0.5" wide (samples had extra yarns removed to have only three yarns in the actual sample) were cut. (Figure 45) Fabric was also used with KM2 Plus® in both directions as reference. The fixture consisted of a metal bottom and top plate covered in a medium grain sandpaper to assist in slippage prevention. Samples are raveled down to three yarns then affixed to rubber gasket strips with an acrylate glue, then topped with another rubber gasket strip. This strip prevented the sand paper from gouging the surface of the fiber and allowed proper pressure to be applied for each sample.

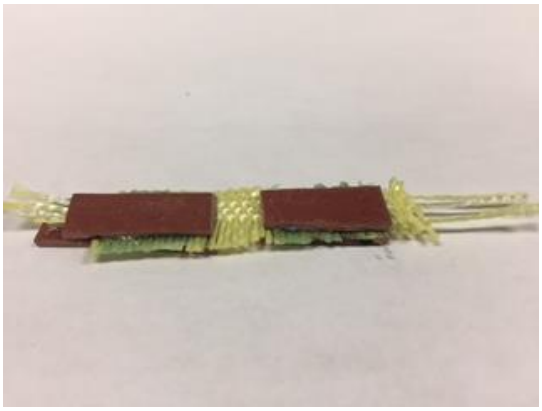

Figure 47 SHPB fabric sample with three yarns sandwiched in rubber gasket tab top and bottom to prevent sample slippage and failure at grip edge.

11.4 SHPB Sample Set up Results and Discussion

Early experimentation to establish best practice for sample preparation included samples with no protection within the grip plate face or at grip edge and samples affixed to paper outside of the gage length. Initial samples utilized five yarns of the desired configuration between the grips. This large number of yarns had more failure at the grip face indicating crowding of the yarn. Air gun pressure was originally set at 0.689 MPa, moved to 0.758 MPa then optimized at 0.621 MPa as samples either had extreme slippage at the higher pressure or exhibited movement in the fixture. The first fixture (Fig 48) used in experimentation was permanently deformed in testing as the design was not robust enough for continued testing.

Figure 48 Initial SHPB sample fixture showing metal failure (highlighted in red) at grip sample bottom plate.

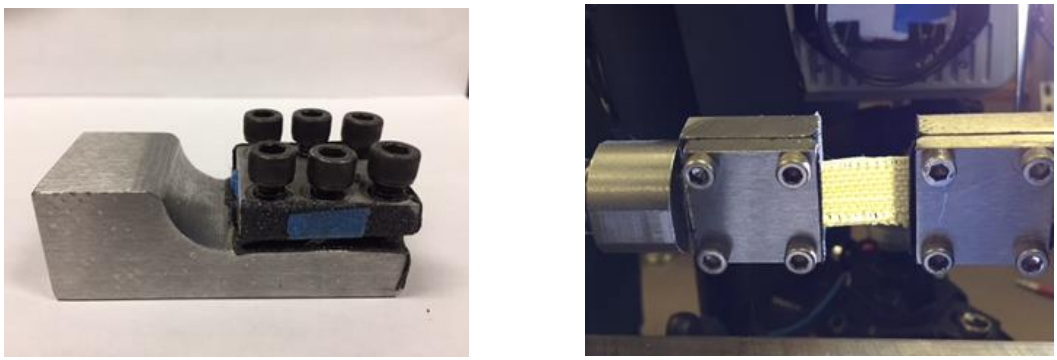

Figure 49 a) Second SHPB sample fixture with more robust design and increase surface area for better sample retention b) sample mounted in fixture

11.5 Experimental Results and Discussion

Analysis of the load is based on dynamic stress equilibrium assumptions. Under quasi-static loading conditions the force is applied slowly, the sample produces a reaction force and maintains equilibrium. Slow application of force gives the sample time to produce a reaction force which is uniform throughout the sample. Under dynamic loading conditions, such as SHPB with strain rates of 1500 – 2500 s^{-1}, the application of force is extremely fast and generates time dependent stress. The sample cannot produce a reaction force until the stress

wave has already passed through the sample. To address this condition the equations must account for the delay, i.e. reflected and transmitted signal. In data analysis we must shift the pulse curves to match the slopes of incident and reflected signals so they align. Equilibrium therefore is only established in the first pull. The remaining pulse signals are not reliable and as such are not included in the calculations for our testing.

Figure 50 shows the pulse orientation and Figure 51 shows the matching of slopes to account for delay in stress wave passing through sample.

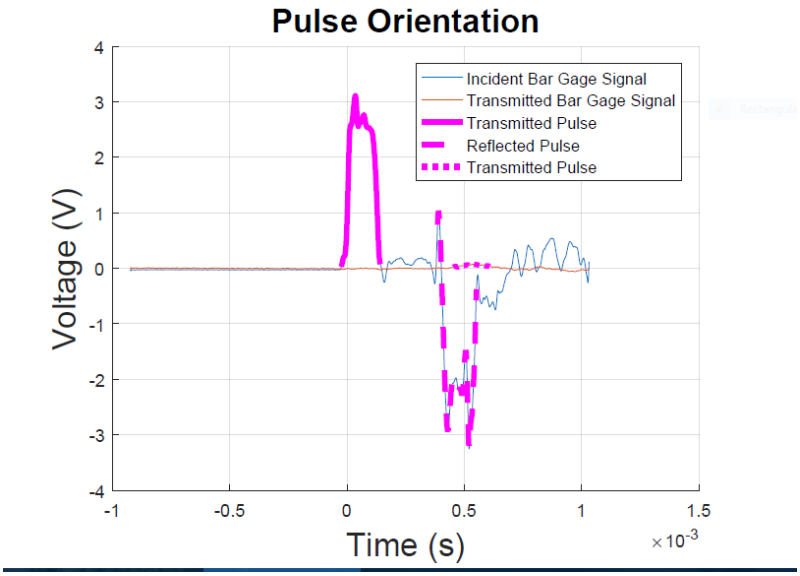

Figure 50 SHPB sample incident and transmitted pulse signal.

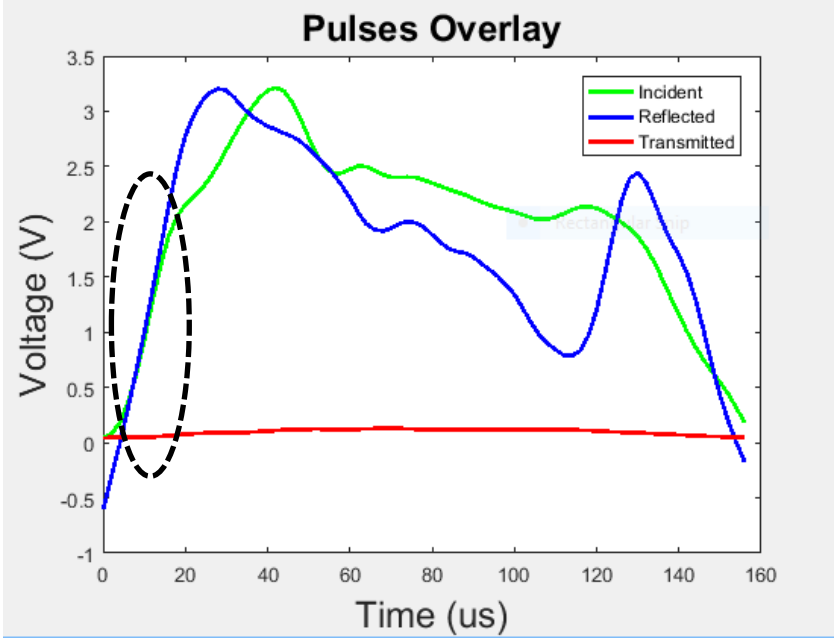

Figure 51 SHPB pulse overlay indicating shift of pulse to match slope of incident and reflected pulse signals. Slope match shown in dashed outline.

Stress strain data was obtained from ten or more samples of each yarn type. Figure 52 shows variation in each yarn type. Alignment in the grips is critical for accurate data. Multiple samples of aramid and commingled fabric were tested intentionally misaligned to evaluate the effect of misalignment. Specimens within the test regime with noted misalignment or slippage at grip edge were removed from the analyzed data. (Figure 53) Misalignment could result in a change to the modulus as the load is not transferred to the yarns equally changing the mode of failure and thus the actual modulus. Modulus change from misaligned samples was over 250 MPa from the reference specimen indicating a significant shift. (Figure 54)

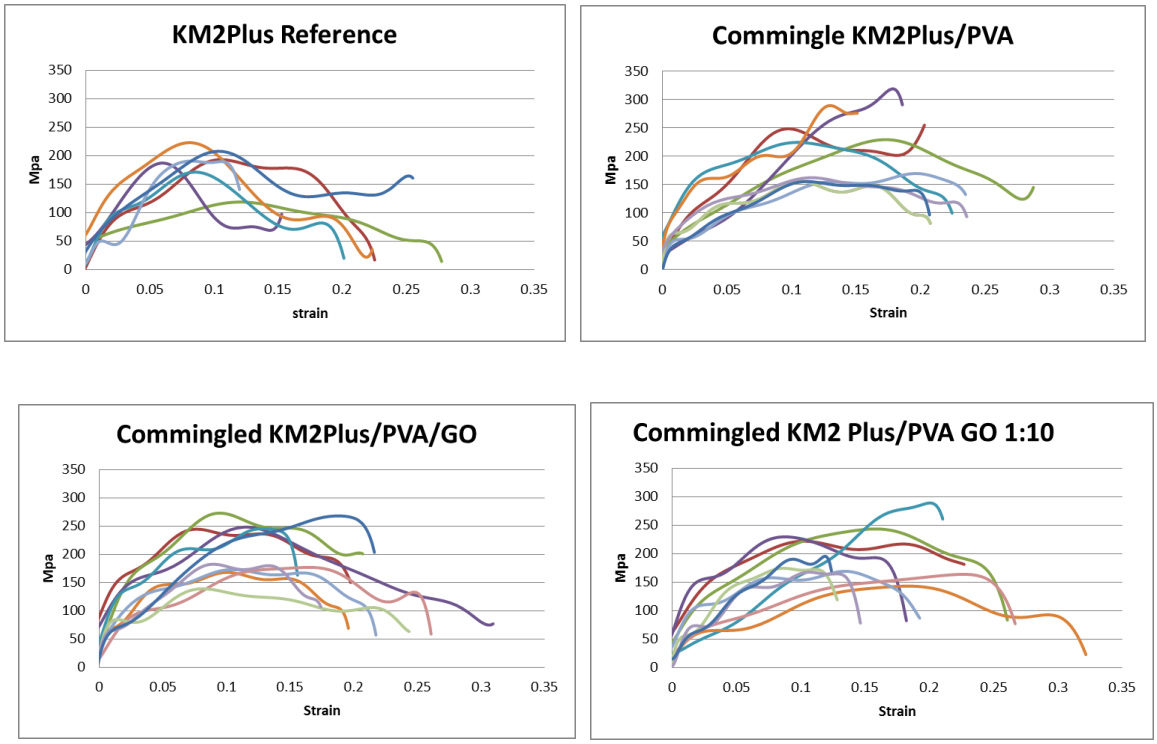

Figure 52 SHPB Stress strain plot of Kevlar reference, hybrid commingled yarn and GO treated hybrid yarns.

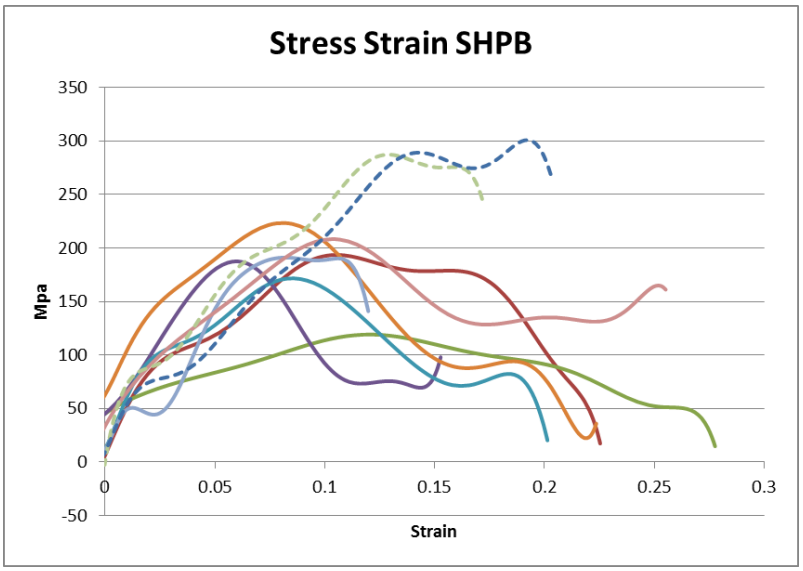

Figure 53 SHPB stress strain curve showing normal sample alignment by solid curves and intentional sample misalignment by dotted lines.

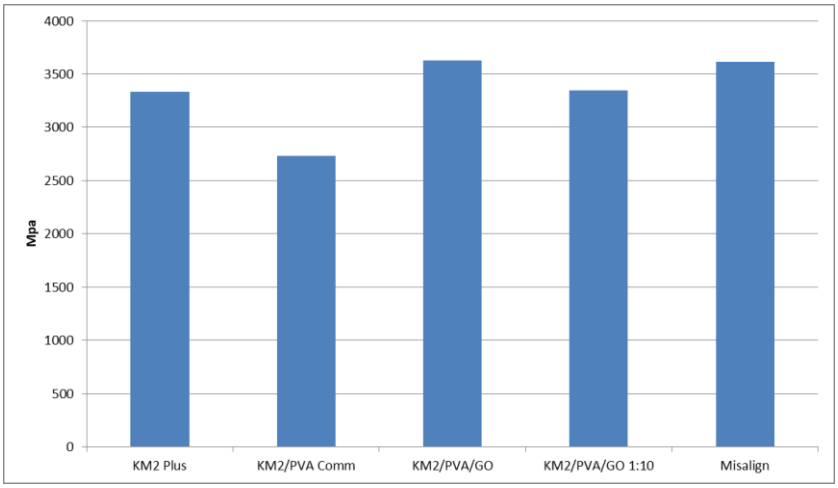

Figure 54 SHPB average modulus calculated from SHPB including intentionally misaligned samples to show effect of alignment during testing.

11.5 Conclusion

SHPB stress stain curves were analyzed in the linear elastic region to determine modulus. Some pretension was present in samples which was evident in initial values in the data set. Tangent modulus was calculated excluding any samples with poor polynomial fit in strain below 0.02.

Modulus of the commingled yarn with GO treatment had the highest modulus followed by the dilute GO treated yarn. The untreated commingled form of KM2 Plus® and PVA had a lower modulus than the reference yarn. This particular trend of commingled yarn having lower strength properties follows that seen in the other test methodologies. The observed stress for the GO treated hybrid yarn was consistently greater than the aramid alone indicating that the incorporation of GO may have a larger contribution in fabric form. There is slightly more elongation in the hybrid commingled fabric specimen with GO and dilute GO treatment. In fabric form the GO may be more constrained and therefore gouges the fiber surface dissipating energy allowing slightly more time for polymer to elongate. The time dependent nature of cumulative damage in the high strain rate event with SHPB may point to GO as having a greater contribution in fabric form. Commingling did not improve modulus as seen in Figure 56. However the yarn with dilute GO treatment was almost equivalent to the aramid further indicating GO contribution in fabric form.

12 SUMMARY CONCLUSION

One purpose of this research was to study hybridization of yarns and introduction of a frictional component to enhance ballistic performance. Differences are seen in the comparison of modulus values obtained from the different methodologies presented in figures 55 and 56. High strain rate testing shifts the linear portion of the stress strain curve based on the ability of the yarn to respond in a viscoelastic manner while quasi-static modulus is the measure of the change in length under tension. The significant difference in modulus of each test methodology may be more indicative of the modulus calculation. In quasi-static testing the modulus is equivalent to cord modulus which looks at a longer section of the stress strain curve while dynamic or high strain modulus typically looks at the initial values on the stress strain curve. Also present in quasi-static testing is a low strain rate which allows the polymer to elongate as seen in Figures 57 and 58. The effect of strain rate may also have a significant role as in dynamic modulus the sample does not experience the same magnitude of strain, as it experiences the sonic pulse propagating through the material. SHPB, with a strain rate above 1000 $s^{-1,}$ has extensive sample deformation (mm to 1-3 cm) until failure. Another objective of this research was to develop additional intermediate level test methodology that may support product development and reduce the need for end item ballistic test. The strain rate effect may dominate the response at high strain rate such that a true comparison between the methods would require extensive testing to validate any correlation.

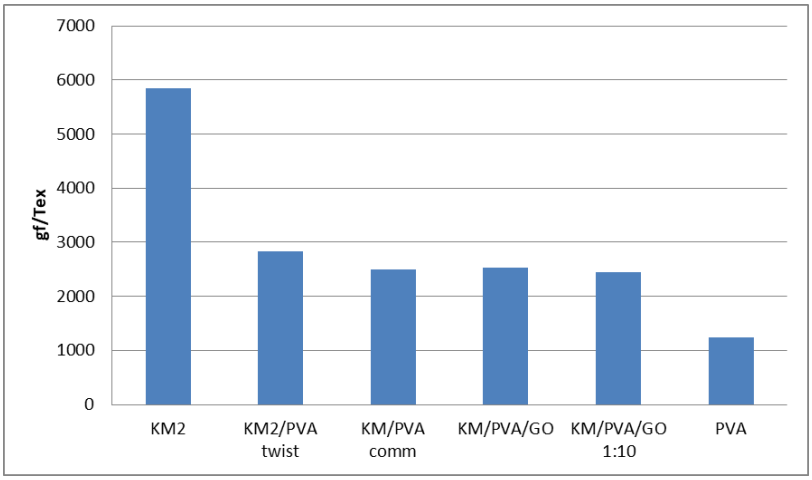

Figure 55 Yarn quasi-static modulus calculated from ASTM D 5035 tensile test method.

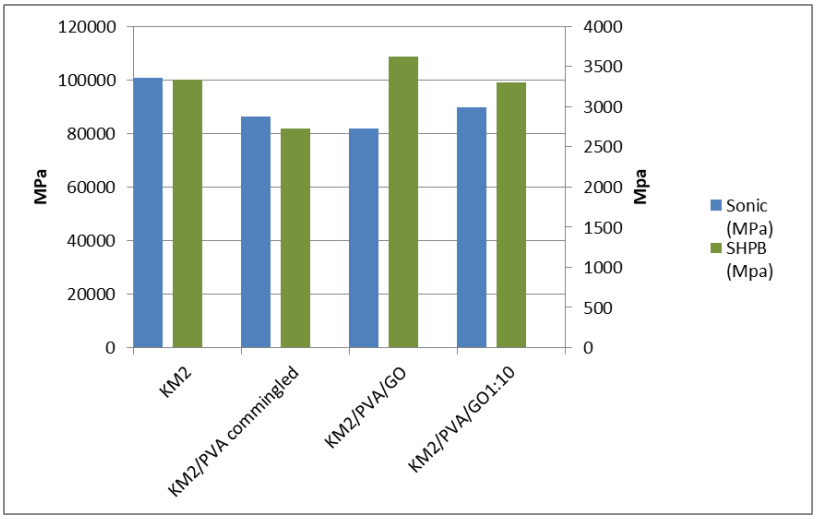

Figure 56 Comparison of modulus of yarn (sonic) and fabric (SHPB) derived from sonic velocity and SHPB tests. See Chapter 9 & 11.

Twisting of the yarn consistently increased the specific strength of the yarn compared to commingling. Commingling of the yarn lowered the ability of the yarn to function as a cohesive unit under stress as is seen in comparison of modulus and toughness. Both methods

however show decreased strength compared to KM2 Plus® yarns. The introduction of PVA did absorb energy as a second break was seen in low strain rate testing. This did not translate into an increase in tenacity or toughness as seen in Figures 31 & 32 for commingled yarn. The increase in tenacity and toughness was observed in the twisted hybrid yarn.

GO treatment on yarns did not increase the ability of the yarn to absorb energy but did show a larger contribution to modulus in fabric even in specimens having the dilute GO application. This contribution may indicate that in fabric form the architecture of the system compliments GO in absorbing energy. Energy must be used to remove the crimp at each yarn intersection increasing the energy dissipation. Yarn specimens with GO treatment did not exhibit an increase in toughness. Further confirmation that GO treatment does not translate to an increase in energy absorption was seen in dynamic modulus as the samples with GO treatment had lower modulus in comparison of all yarn types. GO may act a as a contact surface separator changing the dynamics of surface contact interyarn and intrayarn. This could allow more freedom of movement within the yarn bundle and yarn to yarn. GO platelets may be sliding across each other or smoothing the surface rather than gouging therefore decreasing the energy dissipation. In fabric form movement is more restricted with increased pressure from the constrained system thereby possibly preventing smoothing of the surface causing the GO platelets to gouge the surface increasing energy absorption.

The failure mode in quasi-static testing versus high strain rate as seen in figure 56 showed the aramid had a greater degree of fibrillation at low strain rate. This indicates the ability of the yarn to elongate from intermolecular slipping and respond to the stress absorbing energy. At the high strain rate, as measured with SHPB, the degree of fibrillation was less and of shorter length. PVA showed both brittle and fibrillation modes of failure as noted in the study by

Wang et al. [9] Figure 57 showed the fibrillation and brittle failure modes of PVA. Efforts to identify a stiffer fiber are typically offset with a decrease in breaking strain. The reduction in ductility at some point will dominate the decrease in strain generated on impact yielding a system that has less effective protection at high strain rate.

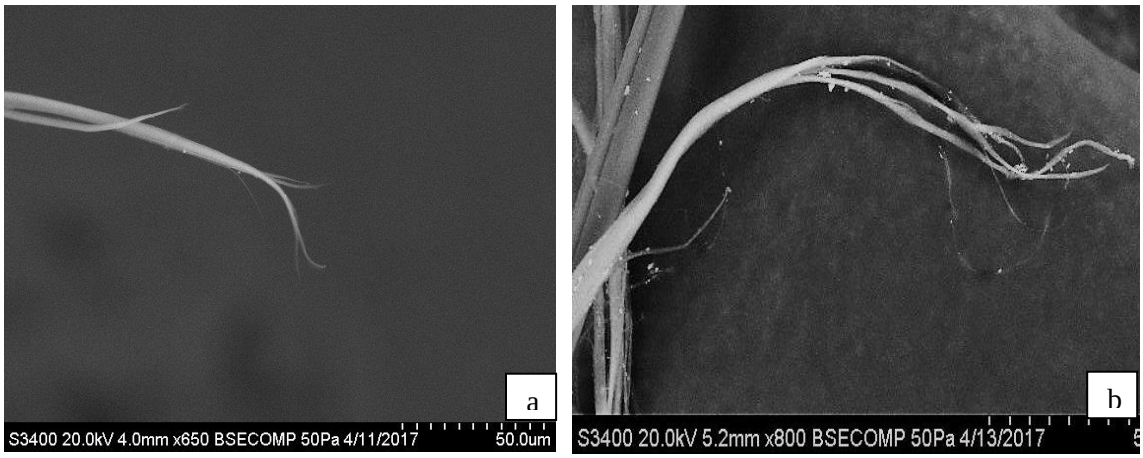

Figure 57 SEM of aramid failure mode in a) SHPB and b) quasi-static testing showing changes in fibrillation

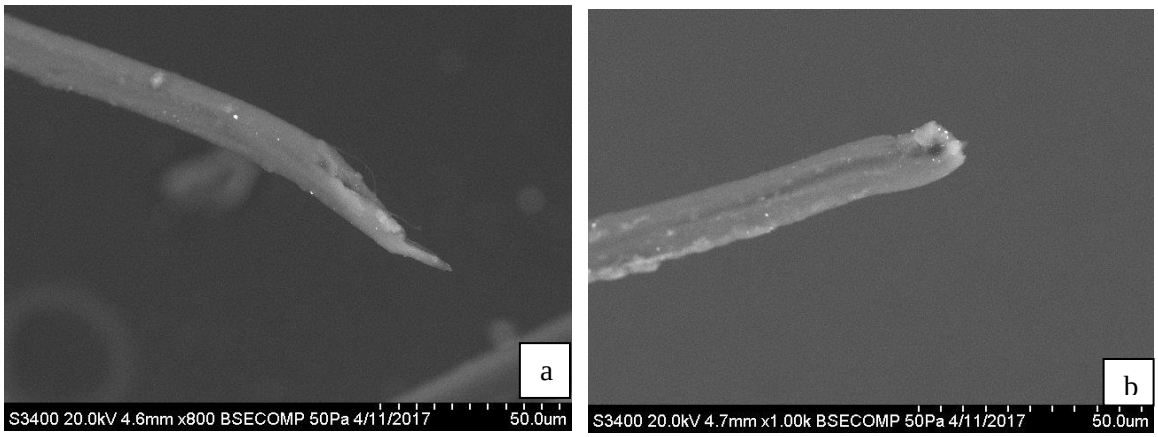

Figure 58 PVA SHPB failure modes a) fibrillation b) brittle failure. Failure in static testing had greater elongation and fibrillation.

The different test methodologies used in this study did not produce consistent comparison of the modulus. Although quasi-static testing compares with current literature values there was poor correlation between the high strain rate methods which would not permit development of a relationship between high strain rate testing and V_{50} testing.

12.1 Recommendations

Yarn testing is more complex at high strain rate as the sample is not a continuous solid. Yarn has multiple filaments and these filaments could be considered as individual elements of the whole with their behavior at high strain rate affected by arrangement within the unit as a whole, overall sample size and length. Further research on multiple yarns rather than single yarn testing with comparison to fabric may produce more thorough understanding of the interactions as most protective systems are multi-element.

Intermediate level testing may provide input on energy dissipation under dynamic loading conditions but sample configuration should be a key component in the research.

Although commingling of yarn to distribute the two yarns more homogenously did not improve yarn toughness, tenacity or modulus, commingling may be more compatible in a composite application. The distribution of the thermoplastic in a consolidated product could produce a functional laminate but could lose strength contribution from the PVA as the temperature in consolidating may cause irreversible change.

Based on the finding that GO does not always contribute as a frictional component further study with fiber surface modification materials need to evaluate their capability of gouging the surface to increase energy absorption.

13 REFERENCES

1. National Institute of Justice: *NIJ Standard-0101.06.*

2. Tonelli, A. Polymers from the Inside Out: An introduction to Macromolecules 2001.

3. About.com , Ellis M. History of Body Armor and Bullet proof vests.

4. Bhatnagar A., *Lightweight ballistic composites*, Woodhead Publishing Limited, Cambridge, 2006.

5. Coffey A.B., O'Bradaigh C.M. and Young R.J.; Interfacial stress transfer in an aramid reinforced thermoplastic elastomer, *J Mater Sci* (2007) **42** 8053-8061.

6. Yue C.Y. , Padmanabhan K.; Interfacial studies on surface modified Kevlar fibre/epoxy matrix composites, *Composites B:Eng* (1999) **30** 205-217.

7. McAllister Q.P., Gillespie J.W., VanLandingham M.R.; The influence of surface microstructure on the scratch characteristics of Kevlar fibers, *J Mater Sci* (2013) **48** 1292-1302.

8. McAllister Q.P., Gillespie J.W., VanLandingham M.R.; Evaluation of the three-dimensional properties of Kevlar across length scales, *J Mater Res* (2012) **27** 1824-1837.

9. Wang Y. and Xia Y.; Dynamic tensile properties of E-glass, Kevlar49 and polyvinyl alcohol fiber bundles, *J Mater Sci* (2000) **19** 583-586.

10. Erkendirci O.F. and Haque B.Z.; Investigation of penetration mechanics of PW Kevlar fiber reinforced HDPE composites, *IJDM* (2012) **22** 304-322.

11. Adams, D., Fiber-matrix interfacial bond test methods Dr. Don Adams, Composites World Jan 2011.

12. Nilakantan G., Merrill R.L., Keefe M. Gillespie J.W. and Wetzel E.D.; Experimental investigation of the role of frictional yarn pull-out and windowing on the probabilistic impact response of Kevlar fabrics, *Composites B:Eng* (2015) **68** 215-229.

13. Grujicic M., Hariharan A., Pandurangan C-F., Yen B.A., Cheeseman Y., Wang Y., Miao Y., Zheng J.Q.; Fiber-Level Modeling of Dynamic Strength of Kevlar KM2 Ballistic Fabric, *J Mater Eng & Perf* (2012) **21** 1107-1119.

14. Zhou X.-F., Wagner H/D.; Fragmentation of two-fiber hybrid microcomposites: stress concentration factors and interfacial adhesion, *Compos Sci & Tech* (2000) **60** 367-377.

15. Pradhan A.K., Alagirusamy R. and Bijwe J.; Tribological properties of aramid-polypropylene composites from commingled yarns: influence of aramid fibre weight fraction, *J Text I* (2009) **100** 702-708.

16. Almusallam T.H., Abadel A.A., Yousef A.A. and Siddiqui N.A.; Effectiveness of hybrid-fibers in improving the impact resistance of RC slabs, *Int J Impact Eng* (2015) **81** 61-73.

17. Dancygier A.N., Yankelevsky D.Z.; High strength concrete response to hard projectile impact, *Int J Impact Eng* (1996) 18 583-599.

18. Kwolek S.L., US Patent, 3671542, 1972.

19. Dubey A., US Patent 7732032 B2, 2004.

20. Tour J.M., Kosynkin D., US Patent EP2432733, 2010.

21. Wang Y., Xia Y. and Jiang Y.; Tensile behavior and Strength Distribution of Polyvinyl –Alcohol Fibre at High Strain Rates, *Appl Compos Mater* (2001) **8** 297-306.

22. Sanborn B., Weerasooriya T.; Quantifying damage at multiple loading rates to Kevlar KM2 fibers due to weaving, finishing, and pre-twist, *Int J Impact Eng* (2014) **71** 50-59.

23. Gao,W., *Graphene Oxide Reduction Recipes, Spectroscopy and Applications*, Springer International Publishing, Switzerland, 2015.

24. Giannopoulos, I., Burgoyne, C., (2009-10), *Viscoelasticity of Kevlar 49 Fibres* Paper presented at 16th Greek Concrete Conference Retrieved December 2016 from CUED Publications database.

25. McCrum, N. Buckley, C. and Bucknail C.; *Principles of Polymer Engineering* ; Oxford University Press, Oxford, 1988.

26. Ozkaya, N et al, *Fundamentals of Biomechanics: Equilibrium, Motion and Deformation*, Sage Publishing, 1999.

27. Ritchie, R.O., ; The conflicts between strength and toughness, *Nature Materials* (2011) **10** 817 – 822.

28. Thanomslip, C. and Hogg, P.J; Interlaminar fracture toughness of hybrid composites based on commingled yarn fabrics, *Compos Sci & Tech* (2005) **65** 1547-1563.

29. Gao, X-L; tensile Test Results of the Dyneema SK76 1500-dtex Yarn and Kevlar KM2 600-denier Yarn at different twist levels. The University of Texas at Dallas, Richardson, Department of mechanical Engineering (2012).

30. Recchia, S. et al; Analytical model of nonlinear twist dependency for Kevlar yarn based on local filament strain, *Acta Mech* (2017) 228 561-574.

31. Shioya, M. et al; Variation of Longitudinal Modulus with twist for Yarns Composed of High Modulus Fibers, Tex Res J (2001) **71** 928-936.

32. Platt, M. M. *Text Res J* 1950 **20** 665.

33. Hearle, J. W. *J Text Inst* 1958 49 T389.

34. Rao, Y. and Farris, R.; A Modeling and Experimental Study of the Influence of twist on the Mechanical Properties of High-Performance Fiber Yarns, *J Appl Poly Sci* (2000) **77** 1938-1949.

35. Miao, M.; Dynamic modulus and strain wave velocity in ballistic fibre strands, *J Mater Sci* (2016) **51** 5939 – 5947.

36. Rebouillat, S. et al; Surface microstructure of a Kevlar aramid fibre studied by direct atomic force microscopy *Polymer* (1997) **38** 2245-2249.

37. Rao, Y.,et al; Structure-property relationship in poly(P-phenylene terephthalamide) (PPTA) fibers *Polymer* (2001) **42** 5937-5946.

38. Ryan, A. and Postle, R.; Application of Sonic Wave Theory to the Measurement of the Dynamic Elastic Moduli of Woven and Knitted Fabrics *Text Res J* (1981) **40** 732 -740.

39. Ballou, J.W. and Silverman,S.; Young's Modulus of Elasticity of Fibers and Films by Sound Velocity Measurements *J Acous Soc Am* (1944) **16** 113-119.

40. Qui, Y. A novel Approach for Measurement of Fiber-on-Fiber Friction; http://www.ntcresearch.org/current/year8/F98-S09.htm

41. Rao, M.P. et al; Modeling the effects of yarn material properties and friction on the ballistic impacts of a plain-weave fabric, *Composites Structures* (2009) **89** 556-586.

42. Liu, L. et al; The yarn-to-yarn friction of woven fabrics ResearchGate Publishing 2016-11.

43. Kalman,D.P. et al; Effect of Particle Hardness on the Penetration Behavior of Fabrics Intercalated with Dry Particles and Concentrated Particle-Fluid Suspensions *Applied Materials & Interfaces* (2009) **1** 2602-2612.

44. LaBarre, E.D. et al; Effect of a carbon nanotube coating on friction and impact performance of Kevlar *J Mater Sci* (2015) **50** 5431 -5442.

45. Seidt, J. D. et al; Tensile Behavior of Kevlar 49 Woven Fabrics over a Wide range of Strain Rates *Dynamic Behavior of Materials* (2011) **1** 187 – 193.

46. Hopkinson, B.A. A method of measuring the pressure in the deformation of a high explosives by the impact of bullets *Philos Trans R Soc A* (1914) **52** 213 – 237.

47. Kolsky, H. An investigation of the mechanical properties of materials at very high rates of loading *Proc Phys Soc B* (1949) **62** 676-700.

48. Harding, J. et al; Tensile testing of materials at impact rates of strain *J Mech Eng Sci* (1960) **2** 88-96.

49. Zhao, H. Material behavior characteristics using SHPB techniques, tests and simulations *Comp & Struc* (2003) **81** 1301-1310.

50. Gomez del Rio, T. et al; Dynamic tensile behavior at low temperature of CFRP using a split Hopkinson pressure bar *Compos Sci & Tech* (2005) **65** 61-71.

51. Pankow, M. et al; Specimen size and shape effect in split Hopkinson pressure bar testing *J Strain Analysis* (2009) **44** 689 -698.

52. Pankow, M. et al; Split Hopkinson pressure bar testing of 3D woven composites *Compos Sci & Tech* (2011) **71** 1196-1208.

53. Tan, V.B.C. et al; Characterization and constitutive modeling of aramid fibers at high strain rates *Int J Impact Eng* (2008) **35** 1303-1313.

54. Torun, A.R. et al; Effect of Twisting on Mechanical Properties of GF/PP Commingled Hybrid Yarns and UD-Composites *J Appl Sci* (2012) **123** 246 -256.

55. Wen Lou, C. et al; Effect of twist coefficient and thermal treatment temperature on elasticity and tensile strength of wrapped yarns *Tex Res J* (2016) **86** 24 -33.

56. Weibull, W.; A Statistical Distribution Function of Wide Applicability *J Appl Mech* (1951) **118** 293- 297.